THESIS AND DISSERTATION
UNIVERSITY OF PUERTO RICO
RÍO PIEDRAS CAMPUS

Using a native insect species and its neuromuscular system as models for assessing water toxicity in Puerto Rico: *Chironomus* sp. "Florida" (Diptera: Chironomidae)

Roberto Reyes Maldonado
Ph.D. Student
Intercampus Doctoral Program
Biology Department
August 26, 2022.

UNIVERSITY OF PUERTO RICO
RÍO PIEDRAS CAMPUS
GRADUATE PROGRAM
DEPARTMENT OF BIOLOGY

CERTIFICATE OF APPROVAL

PH.D THESIS

This is to certify that the Ph.D. thesis of

Roberto Reyes Maldonado

has been approved by the Examining Committee for the thesis requirement for the Doctor of Philosophy degree in Biology at the August 2022 graduation.

Thesis Committee: _____

Bruno Marie, Thesis Supervisor

_____

Alonso Ramírez, Thesis Supervisor

_____

Jorge Ortíz Zayas

_____

Alberto Sabat

_____

William Gregory Cope

Biographical summary of the author

Roberto Reyes Maldonado

Educational Background

2016-2022 Ph.D. Graduate Student
Department of Biology/Intercampus Program
University of Puerto Rico
Río Piedras, Puerto Rico

2011-2016
University of Puerto Rico
Río Piedras, Puerto Rico
B.S.- Integrative Biology

January 2018- Summer 2022
Ph.D. Graduate Student
CREST-PRCEN Program
Neurobiology and Genetics Laboratory
Principal investigator: Bruno Marie, Ph.D.

August 2016-December 2018
Ph.D. Graduate Student
LUQ-LTER Program
Tropical Stream Ecology, Ramírez Lab
Principal investigator: Alonso Ramírez, Ph.D.

Published Work:

Rearing methods and life cycle characteristics of *Chironomus* sp. Florida (Chironomidae: Diptera): A rapid-developing species for laboratory studies.

Roberto Reyes-Maldonado, Bruno Marie, and Alonso Ramírez. Plos One. (2021), 16(2), e0247382. **First author**.

Skin bacterial microbiome of a generalist Puerto Rican frog varies along elevation and land use gradients

Hughey, M. C., Pena, J. A., Reyes, R., Medina, D., Belden, L. K., & Burrowes, P. A. PeerJ (2017), 5, e3688. **Co-Author**

Riparian spider communities as indicators of stream ecosystem condition in the Río Piedras watershed of Puerto Rico.

Roberto Reyes-Maldonado, Jose A. Sánchez-Ruiz, Alonso Ramírez, and Sean P. Kelly. Actualidades Biológicas (2017), 39(107), 58-65. **First author**.

ACKNOWLEDGEMENTS

This work was supported by the Puerto Rico Center for Environmental Neuroscience (PRCEN) under NSF grant-HRD 1736019 and by the NIH-NIGMS grant GM103642 to Bruno Marie. Infrastructure support and service were provided, in part, by the grant U54MD007600 from the National Institute on Minority Health and Health disparities (NIMHD). Monoclonal antibodies were obtained from the Developmental Studies Hybridoma Bank, created by the NICHD of the NIH and maintained at The University of Iowa, 45 Department of Biology, Iowa City, IA 52242.

PERSONAL ACKNOWLEDGEMENTS

I would like to acknowledge all the people who have given me all kinds of support during my formative years in the field of science. First, I thank my mentors, Dr. Alonso Ramírez and Dr. Bruno Marie, who trusted me, accepted me in their laboratory, and have given me their best advice to complete my doctorate. I also thank the Puerto Rico Center for Environmental Neuroscience (PRCEN) for providing me with financial and academic support for 4 consecutive years. To all my laboratory colleagues, thank you for always being there and giving me your unconditional help and friendship. I must specifically thank Taissae Sánchez Medina, who helped me in many of my experiments and supported me in the maintenance of the animals used in this thesis. I thank Dr. Glenivette Zayas, who has been the person in charge of restoring me to sanity in recent years. Thank you for helping me cope and continue with my academic plans when anxiety, procrastination, and perfectionism got in the way. Last, but not least, I would like to thank Christian Bosh, thank you for being there giving me support and for helping me review this thesis.

ABSTRACT

Different species of chironomids have been used as laboratory models to detect toxicity in aquatic environments. This is achieved by studying the response of different molecular and morphological markers in the larvae of exposed animals. The use of cell markers is rarely applied to assess toxicity within these animal models, but their implementation could help to assess toxicity in a more cost-effective way and to detect toxicity before morphological responses appear. With the finality to contribute to the field of toxicology and to emphasize the advantages of using cellular markers to assess toxicity, this thesis seeks to determine the efficiency of the *Chironomus* neuromuscular junction (NMJ) as a cellular marker. In order to evaluate the NMJ as a marker, the larvae of a chironomid species native to Puerto Rico, *Chironomus* sp. "Florida", was studied. First, the life cycle of this chironomid was described and a rearing protocol was presented to manage the larvae under laboratory conditions. Then, the neuromuscular system of the last larval stage of this chironomid was described in order to identify a model NMJ. Once the model NMJ was identified, its effectiveness as a marker of toxicity was evaluated by exposing larvae to high doses of two toxic aquatic pollutants: dibutyl phthalate and lead. The obtained results in this work indicates that the *Chironomus* NMJ is an excellent model for assessing toxicity since quantifiable changes at the number of boutons, muscle area, and density of boutons were observable when the larvae were exposed to contaminants. It is hoped that all the descriptions provided in this thesis will encourage the development of additional studies in the field of toxicology, but also in the field of neuroscience and comparative biology.

Table of contents

List of tables

List of figures

Abbreviations

Aglnx	Abdominal ganglion x
Ax	Abdominal segment x
BMMs	Biochemical and molecular marker
Br	Brain
CNS	Central Nervous System
CTM	Cellular and tissue marker
DBP	Dibutyl phthalate
Dmin	Duration of the immature stage
GluR	Glutamate receptor
HRP	Horseradish Peroxidase
LO	Lateral oblique muscle
LT	Lateral transverse muscle
MFM	Morphological and fitness marker
Mes.g	Mesothoracic ganglion
Met.g	Metathoracic ganglion
NMJ	Neuromuscular Junction
Pb^{2+}	Lead (II) ion
PNS	Peripheric Nervous System

Pro.g	Prothoracic ganglion
SBM	Segmental border muscle
Syn	Synapsin
Tg	Terminal ganglion
Tx	Thoracic segment x
VEL	Ventral external longitudinal muscle
VIL	Ventral internal longitudinal muscle
VNC	Ventral nerve cord
VO	Ventral oblique muscle

CHAPTER I

Introduction

A variety of freshwater organisms have been identified as potential models for bioassays and ecotoxicological analyses. The aquatic larvae of various species of non-biting midges (Diptera: Chironomidae) have been used by environmental agencies and scientists around the world to detect the toxicity and bioaccumulation of sediment and water associated contaminants (Ingersoll et al. 2000). The advantage of using chironomids in toxicology is because these animals are easy to maintain under laboratory conditions, resist environmental changes, feed and burrow in benthic sediments, respond to many pollutants, and have a short life cycle (Ingersoll et al. 2000). A specific genus, *Chironomus*, has been used across the Americas, being the species *C. tentans*, *C. riparius*, *C. decorus* and *C. sancticaroli* the most used as models (Maier et al. 1990, Naylor and Rodrigues 1995, Ingersoll et al. 2000, Rebechi and Navarro-Silva 2012).

A series of markers have been applied to assess toxicity with the larvae of these species, ranging from biochemical and molecular markers (BMMs) (Martinez et al. 2001, Lee et al. 2006) to morphological and fitness markers (MFMs) (Ingersoll et al. 2000, Meregalli et al. 2000). The main benefit of using BMMs to assess toxicity is that this kind of markers show the effects of chemicals before adverse effects are detectable at higher levels of biological organization (Newman, 2014). Also, BMMs can provide important insights regarding how organisms deal with toxic chemicals and the mechanisms of toxicity (Forbes et al. 2006). In the case of MFMs, the main benefit is that the effects observed on individuals can be used to anticipate ecological effects. Despite the benefits offered by

these markers, they also have disadvantages. For example, BMMs are expensive to use in terms of the equipment needed and running costs (Forbes et al. 2006) while MFMs are negatively influenced by the animal behavior and capacity of producing detoxification mechanisms (Newman, 2014).

Although BMMs and MFMs provide important information when assessing toxicity in freshwater environments, cellular and tissue markers (CTMs) represent a better alternative (Richardi et al. 2015). These markers provide information on the integration of changes produced at molecular, biochemical, and physiological level that have resulted from chemical exposure (Férard and Blaise 2013). As a result, contaminant-induced cellular and tissue alterations can be related to health and fitness of individuals allowing further extrapolation to population or community effects (Férard and Blaise 2013). When compared to BMMs and MFMs, CTMs present a most cost-effective way to verify toxicant effects and present better responses to long-term alterations with higher ecological relevance (Richardi et al. 2018).

CTMs have been used as early warning systems for determining potential effects of contaminants at the level of individuals and populations (Newman 2014). Cellular and tissue features, such as cell necrosis, tissue morphological change, and even cancer rate have been used in ecotoxicology to assess and detect toxicity. The use of these types of markers for freshwater toxicology have been performed primarily with fish models, where toxicologist have been able to assess the effects of different types of compounds using the gills and hepatic tissue (Forbes et al. 2006, Newman 2014). Despite the wealth of information on the effects of contaminants on cellular and tissue features, the implementation of this type of markers to assess toxicity with invertebrate models remain

remarkably unused. The practical advantages of using invertebrate models instead of vertebrate models rely in the small size and short life cycle of the models, thus toxicity can be evaluated faster and using less laboratory space (Maciorowski and Clarke 1980).

The larvae of different non-biting midge species have been used for decades to assess water toxicity but as mentioned, cellular markers have not been used with these models when pursuing bioassays. Having notice this gap, Richardi et al. (2015) presented a histological description of the entire anatomy of the species *C. sancticaroli* in order to recommend the use of histological structures as markers. Later, Richardi et al. (2018) used this description to assess toxicity, being able to detect morphological alteration in the midgut, Malpighian tubules, visceral fat body cells, and salivary glands after acute and chronic exposure to Phenanthrene. A limitation of the procedures presented by Richardi et al. (2015) is that the markers are only evaluated qualitatively and not quantitatively. This limitation can be overcome by using a single cellular marker instead of a series of them. The selected marker should be meticulously described, and their components quantified as done in the field of the neurobiology.

The nervous system, as studied in the *Drosophila melanogaster* model, could be used as reference for the implementation of a quantifiable cellular marker for a *Chironomus* species. Structures such as the neuromuscular junction (NMJ), the contact between a motor neuron and muscle fibers (Webster 2018, Rodríguez Cruz et al. 2020), can be quantitatively analyzed by determining the number of synaptic boutons, arborization, among others (Zhong and Chun-Fang Wu 2004). The NMJ in the *Chironomus* larva is responsible for controlling movements related to swimming, respiration, and feeding; behaviors that commonly are affected by contaminants (Gerhardt and de Bisthoven 1995). The NMJ as

studied in the *D. melanogaster* model has been shown to be responsive to contaminants, presenting changes in the number of different neuromuscular features when the flies are acutely or chronically exposed to contaminants (Morley et al. 2003, Xing et al. 2009). Using the *Chironomus* NMJ as a tissue for quantifying CTMs could contribute in the long term to determinate which chemicals target neuronal tissue, what behavioral changes are attributed to neuronal tissue damage, and to what extent the effects of contaminants in the *Chironomus* nervous tissue are comparable to those observed in models that are not used for freshwater toxicology (e.g., *D. melanogaster*).

As the need to perform toxicological evaluations in Puerto Rico increases due to freshwater pollution, it would be relevant to use a *Chironomus* model and a tissue such as the NMJ to detect toxicity in a robust and cost-effective way. Since no *Chironomus* species have been used in Puerto Rico, the evaluation of the NMJ features as CTM will require the selection of a native species, the description of its rearing under laboratory conditions, the characterization of its neuromuscular tissue, the determination of a model NMJ and the assessment of contaminants on the model NMJ. By achieving this, a novel framework of the nervous system of a midge species from Puerto Rico could be able to be presented, the importance of the use of cellular markers in the field of freshwater toxicology could be highlighted, and a quantitative cellular tool could be provided for the early detection of freshwater contaminants.

The main objective of this research is to assess the suitability of the *Chironomus* NMJ as CTM for freshwater toxicity assessment. To achieve this the Puerto Rican native species *Chironomus* sp. “Florida” was used as model. This *Chironomus* species is a potential candidate model because it has a ubiquitous distribution though the island, is

easily collected in the field and can be maintained under laboratory conditions. The first aim evaluated in this thesis was to establish a method for rearing *Chironomus* sp. “Florida” and describe its life cycle under laboratory conditions. This was determined to adapt current exposure methodologies to the biology of this animal and make the results more ecologically relevant. These descriptions also provide a guide for interested researchers to use *Chironomus* sp. “Florida” in their future toxicological studies.

The second aim of this thesis was to describe the neuromuscular anatomy of *Chironomus* sp. “Florida” at the larval stage. The neuromuscular system has not been described in detail in the *Chironomus* group, so we focused on providing the distribution of different ganglia, nerve tracts, muscles and NMJs through the larval tissue. In addition, we provided the necessary nomenclature to identify the main neuromuscular structures. This was addressed in order to identify a model NMJ to use as CTM.

Finally, the effect of environmental, biological, and chemical variables on the nervous system of *Chironomus* sp. “Florida” was addressed using the NMJ as CTM. Knowing the effect of these variables on the NMJ helped to exclude those factors that could potentially interfere with toxicological results during assays while addressing the effects of chemicals helped to validate the NMJ as CTM.

Overall, this research establishes a framework to use the native chironomid species *Chironomus* sp. “Florida” as laboratory model for assessing toxicity using the NMJ as CTM.

CHAPTER 2

REARING METHODS AND LIFE CYCLE CHARACTERISTICS OF *CHIRONOMUS* SP. FLORIDA (CHIRONOMIDAE: DIPTERA): A RAPID-DEVELOPING SPECIES FOR LABORATORY STUDIES

This thesis chapter is part of a published article titled:

Rearing methods and life cycle characteristics of Chironomus sp. Florida (Chironomidae: Diptera): a rapid-developing species for laboratory studies

Running Title: **Chironomus sp. Florida rearing and life cycle**

Roberto Reyes-Maldonado[1,2], Bruno Marie [2,3], Alonso Ramírez[4]

[1] Department of Biology, University of Puerto Rico; Rio Piedras Campus, San Juan, Puerto Rico

[2] Institute of Neurobiology, University of Puerto Rico; Medical Sciences Campus, San Juan, Puerto Rico

[3] Department of Anatomy & Neurobiology, University of Puerto Rico; Medical Sciences Campus, San Juan, Puerto Rico

[4] Department of Applied Ecology, North Carolina State University, Raleigh, North Carolina, United States of America

This manuscript was published by Plos One on February 22, 2021. (https://doi.org/10.1371/journal.pone.0247382)

Introduction

Chironomids are one of the most common insects inhabiting freshwater bodies. The larvae are ubiquitous and can be found in any aquatic environment, from lakes to phytotelmata (Pinder 1995). A great part of the species in this group are benthonic, some of them feeding on sediment, detritus, and other types of organic matter (Berg 1995). Larval morphological characteristics are diverse, and some groups are noticeable by their red color, which is why many of the species are commonly called bloodworms. This coloration is given by a type of hemoglobin, a protein that is used for fixing oxygen and possibly metabolizing some environmental contaminants (Osmulski and Leyko 1986). This characteristic of chironomids and their symbiotic relation with endogenous bacterial communities give them the advantage of tolerating and colonizing polluted environments (Weber and Vinogradov 2001, Senderovich and Halpern 2013).

Despite the larval tolerance to contaminated environments, chironomids are prone to exhibit changes and disruptions at molecular, morphological, and behavioral levels as a response to their interaction with contaminants (De Haas et al. 2005; Azevedo-Pereira & Soares 2010). For this reason, scientists have used them as freshwater bioindicators and laboratory models, taking their tolerance to infer ecosystem conditions and their responses to assess toxicity or chemical interactions. For example, their relative abundance is used in biotic indices (Baptista et al. 2013; Rattanachan et al. 2014); mouth part deformities are used as a marker for toxicity (Meregalli et al. 2000; Al-Shami et al. 2010); and species survivorship are often used to calculate LC50 values for chemicals (Lencioni et al. 2018). The genus *Chironomus* has been used as a laboratory model, in particular *C. riparius* and

C. tentans. These species are ecologically important and are easy to culture under laboratory conditions (Ingersoll et al. 2000). They have been used principally in temperate zones but studies in tropical regions (e.g., Brazil, northern Argentina, and India) recommend the use of local or tropical species, even though there is little information on them (Bhaduri et al. 2012, Rech et al. 2014, Buso et al. 2018). Using local species as models might result in a better alternative as they are adapted to local environmental conditions (Freitas and Rocha 2011).

In the Insular Caribbean, native chironomid species have been used as indicators to infer stream conditions, but not as laboratory models. Researchers have focused on the use of exotic aquatic animals as model organisms for assessing chemical toxicity (e.g., *Danio rerio,* (Colón-Cruz et al. 2018, de León et al. 2020). The information collected from them, however, does not have the appropriate ecological relevance that native species have. Studies have reported using the native species *Macrobrachium carcinus* to assess the effects of chemical pollution (Ortiz Lugo and Sosa Lloréns 2015), but this organism's complex life cycle complicates its maintenance and reproduction under laboratory conditions. The use of a *Chironomus* species could solve these problems since chironomids are easy to maintain and can be found in all freshwater bodies in the Insular Caribbean region (Ferrington et al. 1993, Bello González et al. 2013, Laurindo da Silva et al. 2015).

In Puerto Rico, we have been studying a native *Chironomus* species to determine its use as a laboratory model for assessing toxicity and responses to chemical pollution. The species *Chironomus* sp. "*Florida*" [as provisionally called by Epler (2001)] has several

qualities that make it a potential laboratory model. Indeed, it has a widespread distribution through the central and north-eastern part of the island, its larvae can be found inhabiting the sediments of streams and temporary pools at any time of the year, and all of its stages can be maintained under laboratory conditions. Nevertheless, no rearing protocol and life cycle data have yet been reported to recommend this species as a laboratory model. The present study addresses this lack of information by describing the rearing method that we have developed for *Chironomus* sp. *"Florida"* through 3 years of observations. In addition, we provide details on the life cycle of the species, presenting some effects observed when animals are exposed to different temperatures and food concentrations.

Materials and methods

Field collection and species identification

We initiated all cultures by collecting egg masses in the field, thus securing hundreds of larvae of the same species without major effort. The best method for securing egg masses of *Chironomus* sp. *"Florida"* in Puerto Rico was to place water-filled dark containers in open areas. The water in these containers reflected polarized light, which gravid females used as cues for selecting places to lay eggs (Lerner et al. 2008). Eggs masses were easy to observe on the water's surface, attached to the edge or floating, during the evening and morning 1 to 7 days after placing the containers. They were collected by suctioning with a Pasteur pipette or by detaching and lifting them with the tip of the finger or a small wooden stick. Easily identifiable, this was the only species on the island with straight flat-shaped egg masses (Fig. 2.1).

A residential area in San Juan (18º24’5.02”N, 66º3’11.47”W, 625 meters away from Río Piedras mainstem) was used successfully since 2017 to obtain egg masses with this method. Egg masses of *Chironomus* sp. *“Florida”* also were collected in a more time-consuming way by sweep-netting emerged aquatic plants at Quebrada San Antón, Carolina (18°25’04.7”N 66°00’03.0"W), and by direct collection in temporary pools, artificial channels, and animal watering troughs at Río Bauta, Morovis (18°15’41.4”N 66°27’25.9”W) and Quebrada Buruquena, Río Grande (18°19’17.7”N 65°49’10.9”W).

Egg masses were placed in clean Petri dishes with dechlorinated tap water until hatching. A single species culture of *Chironomus* sp. *“Florida”* was started by placing the larvae from five to ten masses into a single culture aquarium, as described below. Species identity was confirmed at the larval stage using cues described in Epler (2001).

Our *Chironomus* sp. *“Florida”* rearing apparatus consisted of a series of interconnected aquariums with an overflow system (Fig. 2.2). Aquariums were made of plastic, with a capacity of 8 L (29x16x18 cm) (Fig. 2.1), and an aerial enclosure (15.5 cm height) made of two curved wires (50 cm length) intersected and attached at each corner top of the aquarium (Fig. 2.2). Each aerial enclosure was covered with a handmade case of mesh fabric (1 mm pore), held in place with a polyester elastic band and with a straight aperture (15 cm length) on one of the sides sewed and secured with a clasp locker (Fig. 2.3). This aperture provided access to the interior of the aquarium without disturbing the enclosed adults.

The overflow system was made by drilling an aperture (2 cm diameter) in one of the short lateral faces of the aquariums, located at 8 cm from the sides and 9 cm from the

base. PVC elbows were secured to the openings of each aquarium and used as the overflow water outlets (Fig. 2.4). A ring made of plastic canvas (4 cm diameter; 2 cm height) was positioned at the mouth of each outlet to prevent drifting of egg masses, large larvae, and pupae (Fig. 2.5). Additional 2-cm PVC tubing was used to connect the aquariums and drain the water to the filter (Fig 2.6).

The filter was made with a 19 L container (Fig. 2.7), filled with layers of gravel, activated carbon, and sand (Fig. 2.8-10). Water was moved by gravity, exiting through holes at the bottom of the container (Fig. 2.11). A handmade strainer (nominal sieve opening=250 μm) was positioned between the filter and the incoming water to prevent the entry of coarse matter, drifting larvae, and drifting egg masses into the filter (Fig. 2.12). This filter was placed inside a glass aquarium (43x29x38 cm) (Fig. 2.13) provided with 16 L of dechlorinated tap water, aeration, a water pump, and a heater (Fig 2.14-16). The filter was reinforced biologically by adding beneficial bacteria from Imaginarium™ Biological Booster (0.13 ml/L). The water pump inside the aquarium sent the filtered water through a UV filter to decrease the number of bacteria, protozoans, algae, and diatoms (Fig. 2.17). From the UV filter, the water was distributed using PVC pipe (2 cm diameter) equipped with irrigation tubing and micro-spray nozzle valves (Fig. 2.18-19).

Culture apparatus

Our *Chironomus* sp. *"Florida"* rearing apparatus consisted of a series of interconnected aquariums with an overflow system (Fig. 2.2). Aquariums were made of plastic, with a capacity of 8 L (29x16x18 cm) (Fig. 2.1), and an aerial enclosure (15.5 cm height) made of two curved wires (50 cm length) intersected and attached at each corner

top of the aquarium (Fig. 2.2). Each aerial enclosure was covered with a handmade case of mesh fabric (1 mm pore), held in place with a polyester elastic band and with a straight aperture (15 cm length) on one of the sides sewed and secured with a clasp locker (Fig. 2.3). This aperture provided access to the interior of the aquarium without disturbing the enclosed adults.

The overflow system was made by drilling an aperture (2 cm diameter) in one of the short lateral faces of the aquariums, located at 8 cm from the sides and 9 cm from the base. PVC elbows were secured to the openings of each aquarium and used as the overflow water outlets (Fig. 2.4). A ring made of plastic canvas (4 cm diameter; 2 cm height) was positioned at the mouth of each outlet to prevent drifting of egg masses, large larvae, and pupae (Fig. 2.5). Additional 2-cm PVC tubing was used to connect the aquariums and drain the water to the filter (Fig. 2.6).

The filter was made with a 19 L container (Fig. 2.7), filled with layers of gravel, activated carbon, and sand (Fig. 2.8-10). Water was moved by gravity, exiting through holes at the bottom of the container (Fig. 2.11). A handmade strainer (nominal sieve opening=250 μm) was positioned between the filter and the incoming water to prevent the entry of coarse matter, drifting larvae, and drifting egg masses into the filter (Fig. 2.12). This filter was placed inside a glass aquarium (43x29x38 cm) (Fig. 2.13) provided with 16 L of dechlorinated tap water, aeration, a water pump, and a heater (Fig. 2.14-16). The filter was reinforced biologically by adding beneficial bacteria from Imaginarium™ Biological Booster (0.13 ml/L). The water pump inside the aquarium sent the filtered water through a UV filter to decrease the number of bacteria, protozoans, algae, and diatoms (Fig. 2.17).

From the UV filter, the water was distributed using PVC pipe (2 cm diameter) equipped with irrigation tubing and micro-spray nozzle valves (Fig. 2.18-19).

Culture conditions

Each culture aquarium was provided with 4 L of dechlorinated tap water. Water temperature was maintained at 27±1 ºC, which is an average temperature that we have observed for lowland streams in Puerto Rico. Air temperature was maintained at 25±1 ºC by using a 250-watt ceramic heat lamp, simulating the range of average atmospheric temperature reported for the island [24 to 29 °C (Murphy et al. 2011)]. Both temperatures were regulated with digital thermostats. Constant aeration in the filter chamber provided oxygenated water to culture aquariums. A photoperiod of 12:12 dark/light was maintained using 10-watt LED lights with a temperature color of 6400 K.

Substrate and diet

The substrate we use for culturing the larval *Chironomus sp. "Florida"* was based on the methodology given by Batac-Catalan & White (1982). A key difference in methodology is that instead of shredded paper towels soaked in acetone and boiling water, commercial coffee filters made of oxygen whitened paper was used. The bottom of each aquarium was covered with a 2-cm layer of this material. Larvae were fed with a stock suspension made of Tetramin® fish flakes with tap water. The food suspension was prepared in large batches, separated into individual 1.5-ml Eppendorf tubes™, and stored at -40 ºC until use. The larvae in each tank were fed at a concentration of 2 mg/larva (~400 mg/aquarium) of Tetramin® daily.

Reproduction

Since *Chironomus* sp. *"Florida"* is a species that requires swarms to mate, adults were left in the culture aquariums after emergence. The culture aquarium enclosure provided enough space for adults to conglomerate and for males to start swarming behaviors at the beginning and end of the photoperiod. Because males must be more abundant than females for mating to occur, in some instances adults from all culture aquariums were collected and placed in a single aquarium to obtain egg masses. Adults were collected using 50-ml Falcon® centrifuge tubes and a flashlight to attract them into the container. The same method was used to release them into the recipient aquarium.

Culture maintenance

From Monday to Friday, each canvas ring was removed and cleaned under tap water. Floating dead adults and exuviae were left to move down through the overflow outlets for 15 minutes. Any decaying material was brushed and removed. The filter strainer was washed under tap water after cleaning the aquariums to remove all the accumulated material. One to two times a week, 50% of the water volume in the filter aquarium was siphoned and replaced with dechlorinated tap water adjusted at the culture temperature. This helped to compensate for water evaporation. Additional cleaning was provided if signs of stress were observed (e.g., larvae breathing at surface), bad odors were perceived, or overgrowth of bacteria or protozoa was detected. In those cases, all the water of the filter aquarium was siphoned and replaced as many times as needed to recover balance in the system. Every 3 months the sand, activated carbon, and gravel in the filter were rinsed to

prevent clogging. Because larval substrate decreases over time, new shredded coffee filter was added every 3 to 4 weeks as needed.

Life cycle

Life cycle and growth were described following modifications of the methodologies presented by Zilli (2008). Briefly, we collected 45 egg masses from the laboratory colony in a period of 3 days. The eggs in each mass were quantified and incubated at 27 ºC until hatching. The hatching time was recorded, and the unhatched eggs were quantified under the microscope. Newly hatched larvae from 11 egg masses and with the same age were randomly separated into six 1000-ml beakers provided with oxygenated water and 2 cm of shredded paper. These larvae were incubated at 27 ºC and fed daily as described in the *Diet* section above.

Three of the six beakers were selected to determine larval growth and larval stage. Ten larvae were collected daily from each beaker and fixed in 70% ethanol. The head capsule width and total body length of each larva were measured under a dissecting microscope. Larval growth through time was modelled by relating larval body size and time, fitting the result to the best polynomic curve. Larval instars were identified by obtaining the relationship between head capsule width and total body length following the Dyar proportions (Dyar 1890). This method was also used to determine the growth rate between instars. The larvae in the remaining three beakers were left to reach adulthood and observed daily to record pupae presence, adult emergence, and daily adult sex distribution. Life cycle parameters such as the time to egg hatching, egg mass hatching efficiency, mean

duration of each instar, immature development time, and minimum generation time were determined.

Effect of feeding and temperature on larval emergence

Each variable was evaluated using recently hatched larvae from five egg masses, segregated individually into sets of 25 small containers (5 ml) per treatment. Each container was provided with 3 ml of dechlorinated tap water, and we did not aerate the containers, assuming good oxygen diffusion between the water and the atmosphere due to the low water volume. To evaluate the effect of feeding, we fed four larval sets either 0.5, 1, 2, or 3 mg of TetraMin® suspension daily. Five additional larvae per the first three food concentration were grown in a different setting using 20 ml of water instead of three. This was done to see if the experiment could be reproduced at higher water volumes obtaining the same results.

The same setting used in the feeding experiment was used to evaluate the effect of temperature: six larval sets were exposed to either 15, 18, 20, 25, 29, or 35 ºC. In both experiments, water was exchanged daily to decrease water quality deterioration. The larvae were maintained under experimental conditions until adulthood, when time to reach emergence was recorded for each treatment.

Larval biomass

Larvae from different stages and sizes were collected from the colonies and euthanized in water with formalin (5%). Each larva was measured under a dissection microscope from the anterior edge of the head capsule to the posterior end of the abdomen.

Individual larvae were transferred to a pre-weighed 2-cm^2 aluminum sheet, dried at 60 °C for 24 hours, and weighed in an analytical scale (±0.0001 mg). Larval dry body mass was modelled as a function of larval body length using the power model.

Statistical analysis

All models were obtained with the assistance of the statistical software GraphPad PRISM 7.

Results

Chironomus sp. "*Florida"* egg masses had on average 236.98 (n=45; σ=26.87) oval eggs that turn brownish when fertilized. Embryos were visible 12 hours after being laid and developed completely in less than 24 hours when incubated at 27 ºC. Hatching efficiency of egg masses was 95.56% (n=45), and for viable egg masses hatching efficiency of eggs was 98.67% (n=43). After hatching, the larvae stayed in the gelatinous mass and fed on it for 5 to 8 hours before turning planktonic. Larvae passed through four stages or larval instars that were easily identified by morphology or by relating the head width with the body length (Fig. 2.3A). A summary of the values for head width, body length, stage duration, and morphological appearance is presented in Table 1. The average larval developmental time was 11 days (n=899, σ=1.31), with a minimum and maximum of 8 and 14 days.

The pupal stage developed in hours, producing a pharate adult that emerged in less than 24 hours. Emergence took place between day 10 and day 15 from egg deposition (n=899; $\bar{X}$=13.07 σ=1.31): males appeared between day 10 and day 13 (n=309, $\bar{X}$=11.52

σ=0.64); females between day 12 and day 15 (n=590, $\bar{X}$=13.88, σ=0.70). With this, the average duration of the immature stage was 13 days (n=899, σ=1.31), with a minimum and a maximum of 9 and 14 days. In high humidity environments (86% humidity) males survived an average of four days (n=24; σ=1.47) after emerging, while females survived an average of six days (n=20; σ=1.45). Oviposition was observed from day 13 to day 18, producing a new generation from day 13. The complete overlap and duration of stages is illustrated in Fig. 2.3B.

Animals that were fed at a food concentration of 0.5 mg/larva/day presented shorter adult emergence times than those fed at a higher concentration (Fig. 2.4A). These results were not reproducible at a higher water volume since inverse results were obtained, in that the larvae fed at 2 mg/larva/day were the ones that presented shorter emergence times (Fig. 2.4B). Larvae food deprivation was observed in the 0.5, 1, and 2 mg/larva/day treatments for both water volumes. Deprivation occurred first at low food concentrations and later at high food concentrations (Table 2).

Rearing larvae at temperatures as low as 15 ºC lengthened the time for adult emergence (Fig. 2.4C). As the rearing temperature is increased, emergence time shortened. According to our model, larvae reared above 29ºC are expected to begin to show an increase in the time of emergence. Both, feeding concentration and temperature presented a polynomial relationship with emergence time (Fig. 2.4).

Larval growth at 27 ºC from the first instar larva to the prepupae stage was best represented by using a polynomial model (Fig. 2.5A). This growth model showed a rapid increase in larval size until reaching the ninth day, when growth started to decrease. Growth

rates between instars increased slightly through time, with the last stage being the one with the highest growth rate value (Table 1). The relationship between body length and dry mass was best explained using the power model, rather than linear or quadratic models (Fig. 2.5B).

Discussion

Our method was the result of 3 years of observations on the suitability of different methodologies, including modified versions of Biever (1965), New et al. (1974), and Batac-Catalan & White, (1982). The preference of collecting eggs for establishing new colonies and studies is common and favored by various authors (e.g., Canteiro & Albertoni, 2011; Corbi & Trivinho-Strixino, 2006; Rech et al., 2014; F. Zilli et al., 2009; F. L. Zilli, 2008). With the proposed recirculated system, egg masses can be used to produce and maintain robust colonies without effort for a period longer than 9 months. Although recirculated systems are not commonly used for rearing and maintaining chironomids owing to larval drifting problems, it has the advantage of producing a constant oxygenated, clean, and biologically uncontaminated environment that reduces maintenance time. In our experience, rearing methods such as the ones presented by Biever (1965), Batac-Catalan & White, (1982), and Ingersoll et al. (2000) do not provide long-term stability, and colonies start to present problems with overgrowth of microorganisms with subsequent anoxia, something that is rarely observed with recirculated systems.

We exchanged the material used as substrate by Batac-Catalan & White (1982) since shredded coffee filters offer a fiber like medium that is easy to prepare. This media has a high acceptance by larvae and is used as burrowing and case construction material.

The only disadvantage of this substrate is that it starts degrading into a fine material, hindering its posterior reuse by the larvae.

Tetramin® flakes have often been used to feed larvae (Naylor and Rodrigues 1995, Ristola et al. 1999, Fonseca and Rocha 2004, Corbi and Trivinho-Strixino 2006). Although other rearing methodologies have used a range of feeding sources (e.g., vegetative organic matter, animal chow, manure, algae, and yeast), the use of Tetramin® has been shown to provide larvae with essential amino acids that promote enhanced growth rates in laboratory cultures (Abashy 2005). It is important to mention that our proposed feeding concentration is based on observing how much food the larvae were able to ingest daily. Therefore, further studies are necessary to determine possible effects of the feeding concentrations on reproduction, survivability, and biomass. As in other rearing methodologies, adults were not fed in our method. This approach is based on the idea that adults are short lived and mostly rely on energy obtained during the immature stages to reproduce (Tokeshi 1995).

Our recommended method of aerial reproduction is the optimal way to achieve mating of adults in this species. Other methods, such as confined reproduction chambers, cannot be used since adults need space to swarm to achieve mating. This aerial method has been used elsewhere to keep producing new laboratory generations of species with swarming mating behaviors (Maier et al. 1990, Nath et al. 2009, Bhaduri et al. 2012). This method has provided us with a productivity of more than 15 egg masses/day per rearing unit once colonies are established. The recommended environmental conditions (27 ºC; photoperiod 12light:12dark) are similar to those observed in the wild environment of the species and are in accordance with other methodologies from tropical regions (Peck et al.

2002). Nevertheless, it is important to highlight that these conditions are not necessarily the optimal ones for obtaining high biomass and progeny outputs.

Life cycle

The life cycle of most species in the genus *Chironomus* is similar and is characterized by an embryo enclosed in a gelatinous mass, four larval stages, a pupa, and an adult (Armitage et al. 1995). Egg masses of *Chironomus* sp. "*Florida*" are small (about 236 eggs) relative to other species. Common tropical species of *Chironomus* laid over 350 eggs/mass [e.g., *C. calligraphus*, 369-374 eggs/mass (Rech et al. 2014)], reaching up to 3,300 in some species (Nolte 1993, Sahragard and Rafatifard 2010). The low number that we found is consistent with the medium body size of adult *Chironomus* sp. "*Florida*", as small species are expected to lay fewer eggs per mass (Sahragard and Rafatifard 2010).

Despite the smaller number of eggs in our species, it exhibits an excellent reproductive output based on the number of hatching eggs (98.67%). This high value is in accordance with other species such as *C. riparius* (97.78%) (Sahragard and Rafatifard 2010) and *C. pulcher* (99%) (Dejoux 1971). Hatching starts in less than 24 hours, contrasting with *C. calligraphus* (3 days at 21.8 ±3.2 ºC) (Zilli 2008), *C. xanthus* (1.25 days at 30 ºC) (Trivinho-Strixino and Strixino 1989), and *C. riparius* (2-6 days at 26 ºC) (Sahragard and Rafatifard 2010). This faster embryo development could represent an adaptive advantage to increase fitness, as this species inhabits temporary habitats. The typical egg mass feeding and planktonic behavior after hatching are preserved in this species, a topic that has been observed and discussed elsewhere (Hein and Mahadeva 1992, Fonseca and Rocha 2004, Rech et al. 2014).

Chironomus sp. *"Florida"* has a short life cycle, with a minimum duration of the immature stage (D_{min}) of only 9 days at 27 ºC. This is comparable to other tropical species that have presented similar D_{min} values in a range of the temperatures of 24-30 ºC such as *C. strenzkei* [D_{min}= 10 days (Fittkau 1968)], *C. sancticaroli* [D_{min}= 15 days (Strixino and Strixino 1985)], *C. xanthus* [D_{min}=13 days (Fonseca and Rocha 2004)], *C. calligraphus* [D_{min}= 11 days (Rech et al. 2014)], *C. crassiforceps* [D_{min}=10 days (Peck et al. 2002)], and *C. ramosus* [D_{min}=15 days (Chockalingam et al. 2006)]. As noted for egg hatchability, this low D_{min} could be explained as an advantage for inhabiting temporary habitats.

We used the Dyar proportions to identify the four larval stages, determine growth rate, and obtain stage durability values. This method has been recommended as head measurement ranges are distinctive through each larval stage, something that is not observed with body measurement ranges (Frouz et al. 2002, Fonseca and Rocha 2004, Zilli 2008). In general, head size ranges and growth rates reported in this study for each larval stage are higher than those reported for other tropical species [e.g., *C. crassiforceps* (Peck et al. 2002), *C. sancticaroli* (Strixino and Strixino 1981), and *C. xanthus* (Fonseca and Rocha 2004)]. The average duration of each larval stage is dissimilar from the other stages, increasing every time the larva moves to its next phase. The last larval stage is therefore longer than the previous ones. This situation has been reported for other species, and it has been explained by Tokeshi (1995) as a way to acquire the necessary energy for swarming activity in adulthood.

The larval growth model for *Chironomus* sp. *"Florida"* presents an increment in body size during the initial stages until reaching a period of slow growth at the final larval stage. This kind of growth has been reported in species under the *Chironomus* group (Zilli

2008), but also in species of other genera, such as in the *Goeldichironomus* group (Corbi and Trivinho-Strixino 2006, Zilli et al. 2009). In this growth model, we can observe two unusual behaviors: 1) as larvae age, the variability in larval body size increases; 2) as the larvae in the cohort reach a maximum in growth, a decrease in body size is observed afterward. In the case of the first observation, the dissimilarities in body size could be produced by sexual dimorphism (Richardi et al. 2013)and by intraspecific competition for food and space (Biever 1971). For the second observation, a decrease in body size could be explained by the appearance of the prepupae, a stage characterized by a decrease in thoracic length due to increased swelling. It is important to note that the growth models presented by Corbi & Trivinho-Strixino (2006), F. L. Zilli (2008), and F. Zilli et al. (2009) do not show this decrease. Our observation may result from the use of a different statistical model in our study.

It is important to take into consideration that males and females were not separated to produce the growth curve presented in Fig. 2.5B. This detail is something that this study and other studies have ignored when executing this kind of model because of the complexity of identifying the sex at the larval stage. By constructing models by sex, we could reduce variability and develop more precise growth curves that eliminate the effect of sexual dimorphism.

The pupal and adult stages in chironomids are in general short, ranging from hours to a few days (Armitage et al. 1995, Cranston 2004). The pupa of *Chironomus* sp. *"Florida"* is not an exception, presenting a developmental time of hours (less than 24) similar to *C. crassicaudatus* [22-27 hours at 27 ºC (Frouz et al. 2002)] and *C. riparius* [24 hours at 26 ºC (Sahragard and Rafatifard 2010)]. The longevity of adults in this species

was unexpectedly longer (more than 2 to 3 days), something rarely reported for tropical species. Our longevity values could be the consequence of our experimental conditions provoking restricted flight and reduced dehydration (due to the way we contained the animals). This is confirmed by studies in chironomids and other insects that have demonstrated how decreasing flight and dehydration increase survivability (Benoit et al. 2007, Gibbs and van Dyck 2010).

Effect of temperature and feeding on adult emergence

Temperature and food availability are two variables known to control larval development in chironomids (Maier et al. 1990, Ristola et al. 1999, Sahragard and Rafatifard 2010). Regarding adult emergence, it has been shown that both variables interfere in the duration of this process (Péry and Garric 2006). Typically, adult emergence time is shortened by an increasing rearing temperature, but the emergence time may slightly increase again if the temperature rises above 30 ºC. This decreasing adult emergence time behavior is present in *Chironomus* sp. *"Florida"* This species, however, presents a low tolerance to high temperatures since no survivorship was achieved at 35 ºC. This was unexpected given that this species inhabits the tropics and other species of chironomids can survive in temperatures above 35 ºC (Stevens 1998).

Food deprivation is known to have several effects on chironomids, from changes in fitness to changes in life cycle parameters (Ristola et al. 1999, Péry et al. 2002). The results obtained at low water volume were surprising since an increase in emergence time was expected. Notably, these data were not reproducible at high water volumes, a finding that led us to conclude that the observed behavior at small water volumes was caused by oxygen

depletion related to bacterial overgrowth due to excess of uneaten food. Confirmatory evidence was observed after each water change in the treatments where food concentrations were greater than 1 mg/larva/day. In this case, larvae were observed at the water surface producing constant breathing movements. This behavior was not observed in experiments with large water volumes and high food concentrations where larvae were observed at the bottom of the container with no observable breathing behavior. Although other feeding experiments have mentioned that larvae fulfil nutritional demands at concentrations as low as 0.12 mg/larva/day (Ristola et al. 1999), here we observed that, in a species that grows fast, concentrations of 2 mg/larva/day are required to avoid food deprivation. Nevertheless, in order to achieve faster adult emergence times, it is necessary to avoid unacceptable water conditions due to oxygen depletion and waste production.

In summary, this study showed that a native non-biting species of the *Chironomus* genus could be easily reared under laboratory conditions in Puerto Rico. The native species *Chironomus* sp. *"Florida"* is ideal for this purpose, since it is easy to obtain in the field, easy to maintain under laboratory conditions, and has a short life cycle. The use of a native species model for freshwater toxicological evaluations provides a better understanding of how contaminants affect tropical ecosystems.

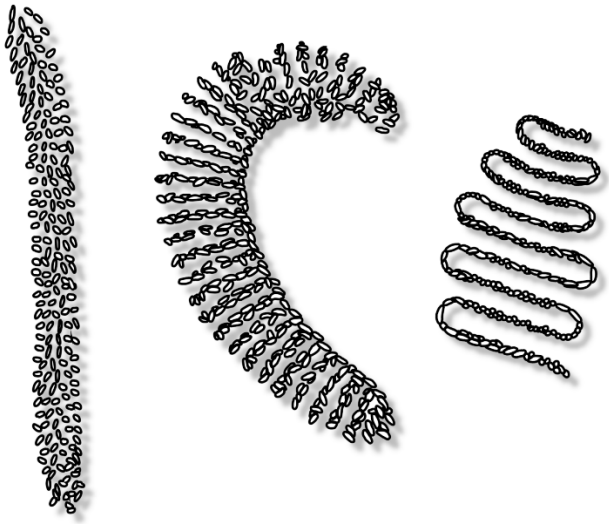

Figure 2.1. Morphological diversity of chironomid egg masses collected in the field. (Left) *Chironomus* sp. “Florida”. (Centre) *Chironomus* sp. (Right) *Dicrotendipes* sp.

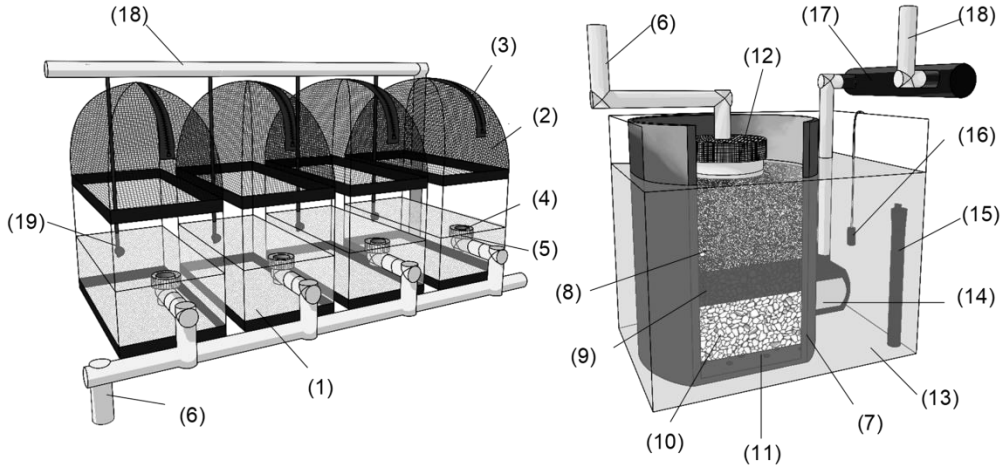

1. Glass aquarium (29 x 16 x 18 cm)
2. Aerial enclosure
3. Clasp lock
4. Outflow pipe to filter chamber
5.Overflow ring
6. Rearing system to filter water pipe
7. 19L container
8. Sand
9. Activated carbon
10. Gravel
11. Drainage
12. Sieve
13. Glass Aquarium (43 x 29 x 38 cm)
14. Water pump
15. Heater
16. Air stone
17. UV sterilizer
18. Water distribution system
19. Flow valve

Figure 2.2. System used for the rearing of *Chironomus* sp. "*Florida*". (Left) Rearing units components. (Right) Filter chamber components

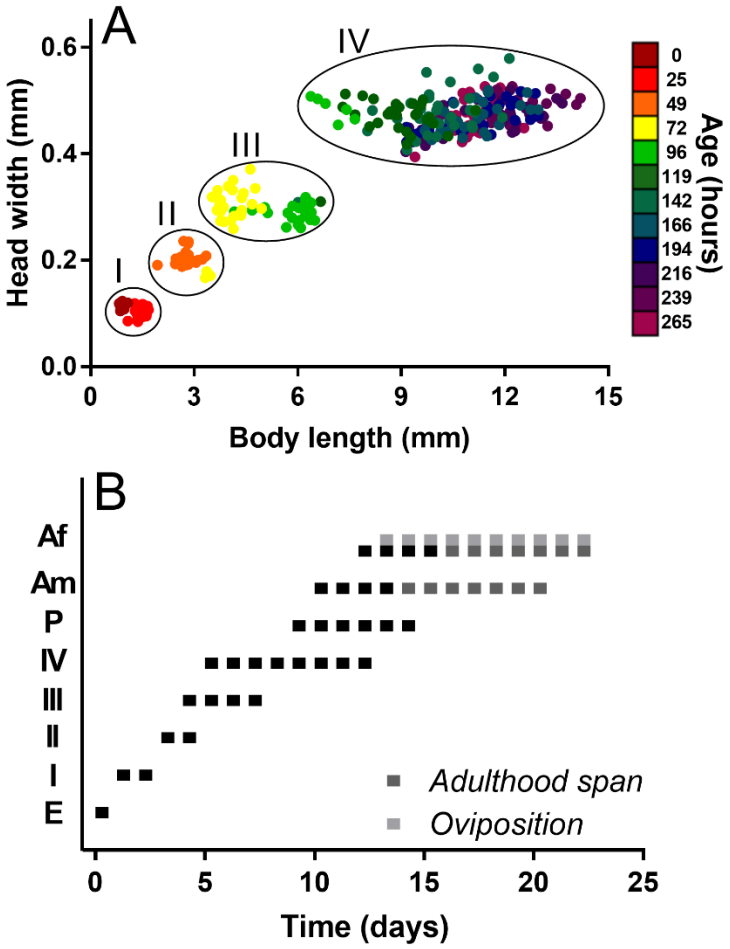

Figure 2.3. *Chironomus* sp. "Florida" stages. (A) Larval stages (I to IV) based on the relation between the head capsule width and body length. (B). Average duration and overlap between stages. Abbreviations: E: embryo; I-IV: larval instars I to IV; P: pupa; Am: adult male; Af: adult female. Adult presence without occurring emergence or adult span is represented in dark grey. Oviposition period is represented by light grey.

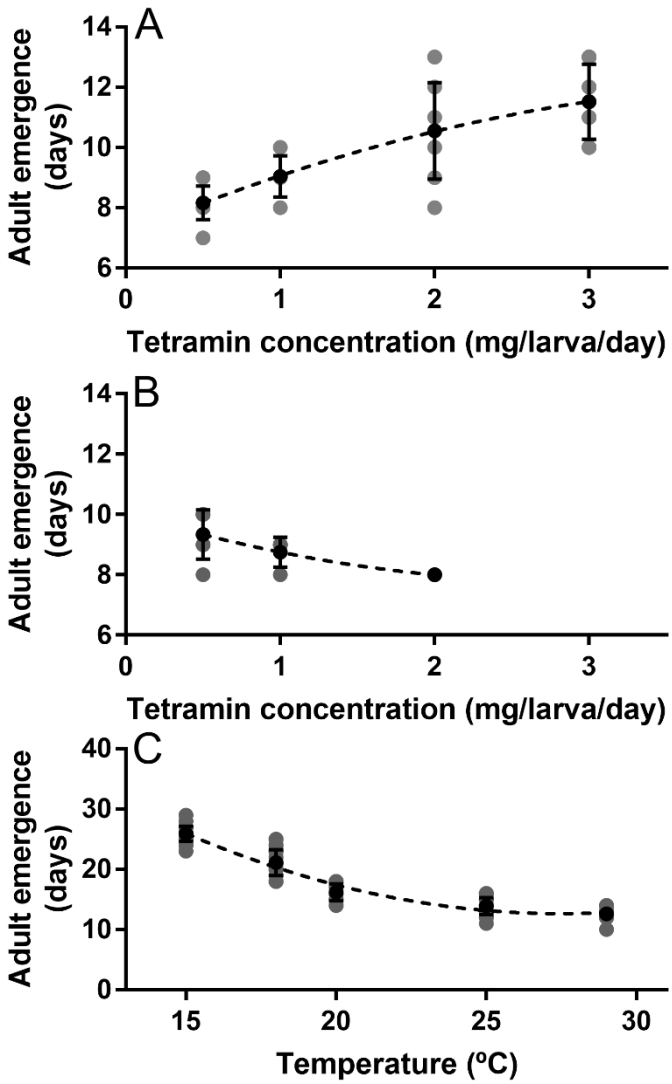

Figure 2.4. Effect of feeding and temperature on adult emergence. (A) Emergence curve obtained from larvae fed at four food concentrations in a water volume of 3 ml. (B) Emergence curve generated from larvae fed at three food concentrations in a water volume of 20 ml. (C) Emergence curve obtained from larvae reared at five different temperatures. Average emergence times and standard deviations are represented in black; individual emergence values are represented in grey. Each Polynomial model can be expressed as (A) $y = -0.24x^2 + 2.17x + 7.12$, R^2=0.60; (B) $y = 0.28x^2 - 1.58 + 10.05$, R^2= 0.54; (C) $y = 0.08x^2 - 4.69x + 77.13$, R^2=0.98

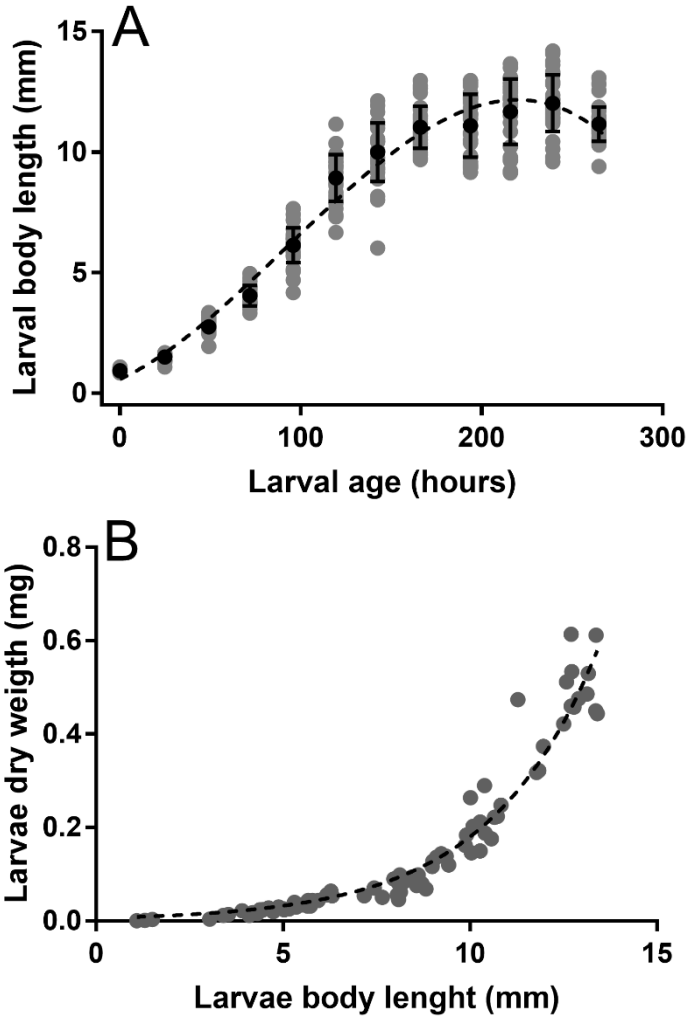

Figure 2.5. Growth and dry biomass equivalence of the larval *Chironomus* sp. "Florida". (A) Relationship of body size and age. (B) Relationship between body size and biomass. Average values and respective standard deviations are represented in black while individual measurements are represented in grey. The polynomial and power regressions can be expressed respectively as (A) $y = -1.37e^{-6}x^3 + 0.24x^2 + 0.35e^{-3}x + 0.34$, R^2=0.94; (B) $y = 0.006e^{(0.34*x)}$, R^2=0.94

Table 2.1. Stage description, life cycle parameters, larval size ranges and larval growth rates of *Chironomus* sp. "*Florida*"

Stage	Description	Life cycle parameters		Larval size ranges		Larval growth rates	
		Day of appearance	Average duration (day)	Head width range (mm)	Body length range (mm)	Head	Body
Embryo	Brownish and oval, secured in gelatinous matrix with other embryos.	0	<1				
Larvae							
Instar I	Clear and planktonic	1	1.71±0.49	0.09-0.12	0.83-1.68	2.02	1.50
Instar II	Whitish coloration	3	3.14±0.29	0.17-0.24	1.94-3.47	2.13	2.22
Instar III	Pink coloration	4	4.55±0.63	0.23-0.37	3.52-6.67	2.18	5.74
Instar IV	Bright red larvae, green coloration can be observed in the thoracic capsule when ready to emerge. Females larger than males.	5	8.90±2.10	0.39-0.58	6.38-14.19		
Pupa							
Male	Bright red or green with evident thoracic horns. Swim actively before emergence. Females bigger than males.	9	1				
Female		11	1				
Adult							
Male	Bright green. Male with plumose antenna and slender abdomen.	10	3.63±1.47				
Female	Females with simple antenna, and brownish and broad abdomen	12	5±1.45				

Table 2.2. Time to food deprivation at different water volumes for each feeding treatment

Food concentration (mg/larva/day)	Time to food deprivation at a water volume of 3ml (days)	Time to food deprivation at a water volume of 20ml (days)
0.5	3	2
1	4	4
2	6	6
3	Not observed	-

CHAPTER 3

THE NEUROMUSCULAR SYSTEM OF *CHIRONOMUS* SP. "FLORIDA": A PROSPECT TISSUE FOR THE CHARACTERIZATION OF QUANTIFIABLE CELLULAR MARKERS.

Introduction

Many morphological features of the *Chironomus* larvae have previously been described (Miall and Hammond 1900, Richardi et al. 2015, Ospina-Pérez et al. 2019) . Miall and Hammond (1900) have presented one of the most outstanding internal anatomical descriptions for all stages of a *Chironomus s*pecies, describing the different cells, tissues and organs that compose the different systems of the studied chironomid. Recent studies have provided new anatomical descriptions using modern histological techniques with the purpose of identifying new cellular and tissue markers (CTMs) for the assessment of freshwater contaminants (Richardi et al. 2015, Ospina-pérez et al. 2019). The anatomical descriptions presented in these recent studies are general and do not share the level of details shown by Miall and Hammond (1900).

The neuromuscular system, a potential system to evaluate contaminants, has not yet been described at detail in the *Chironomus* tissues. Separate descriptions of the musculature or the nervous system have been presented by Miall & Hammond, 1900, Ospina-pérez et al., 2019 and Richardi et al., 2015 as part of their histological descriptions on the *Chironomus* larva. The musculature has been described in a general way and no author has presented the anatomy in its entirety or have assigned a terminology to differentiate the different muscles (e.g., Miall and Hammond 1900). The nervous system has been described

at the level of the central and peripheral nervous system showing the different ganglia (e.g., Miall & Hammond, 1900; Ospina-pérez et al., 2019; Richardi et al., 2015) and their related main nerves (e.g. Miall & Hammond, 1900). Other studies have focused on describing the ultrastructure of the neural sheath, glial cells and neurons, while others have identified the location of selected transmitters, transmitter related enzymes and neuropeptides through the ganglia and alimentary canal (Scales and Credland 1978, Johansson et al. 1986, Robertson et al. 2014). Nevertheless, no study has described the innervation of the different muscles by their respective nerve branches and terminals. A complete description of the neuromuscular system should considerate a detailed muscles characterization and their corresponding nervous innervations.

Because they are easily accessible, documenting the neuromuscular junction (NMJ), the connections between motor neurons, and muscle fibers (Webster 2018, Rodríguez Cruz et al. 2020), could provide a way to quantify and assess the toxicity of the animal milieu. NMJs, which are responsible of inducing muscle contraction and the animal's locomotion (Rodríguez Cruz et al., 2020), have been extensively studied in fruit flies (Menon et al. 2013), crustaceans (Atwood and Cooper 1996), frogs (Letinsky and Morrison-Graham 1980), and mice (Lyons and Slater 1991). A feature of interest to use for assessing toxicity associated effects in the NMJ are the synaptic boutons, rounded structures at the terminal responsible for releasing neurotransmitter to the postsynaptic area in the muscle (Collins & DiAntonio, 2007). Quantification of synaptic boutons number and muscular parameters such as the muscle area could be used as CTMs to detect toxicity induced changes, but the lack of a detailed description of the neuromuscular system has not made it possible.

To contribute with a more complete description of the neuromuscular system, this study presents the neuromuscular anatomy (muscles, nerves and NMJs) of the first abdominal segment in the larvae of the neotropical chironomid *Chironomus* sp. "Florida". This description has been achieved by using immunohistochemical markers used for the visualization of neuromuscular structures in the *D. melanogaster* tissue. Additionally, this study shows a model NMJ that has been selected and described for quantifying features such as synaptic boutons and muscle area. We aim to present these descriptions to provide a most complete vision of the neuromuscular system in chironomids and establish a framework for the study of the *Chironomus* NMJ as a CTM for future toxicological studies.

Methods

Larvae used in this study were acquired from laboratory-reared colonies at the Institute of Neurobiology, University of Puerto Rico. These colonies were obtained from egg masses collected in the field using the methodology presented by Reyes-Maldonado et al 2020. Midges were fed at 2 mg individual^{-1} day^{-1} and maintained at 27ºC with a photoperiod of 12:12 light/dark. The 4th larval instar was the stage used for all the descriptions presented in this study. They were identified by their size (6-14 mm approximately) and bright red coloration (Fig. 3.1a).

Tissue preparation and characterization

Dissection

Tissue was dissected following an adapted methodology described by (Sanhueza et al. 2016). Briefly, 4th instar larvae were attached dorsal face up to a Sylgard dish by pinning

the space between the head and first abdominal segment and the last abdominal segment. Subsequently the larvae were covered with Ringer's saline solution (70mM $NaCl_2$, 4mM KCl, 43mM $MgCl_2$, 10 mM $NaHCO_3$, 115mM Sucrose, 5mM HEPES) and dissected using microdissection scissors under the stereoscope. A first incision was made horizontally above the heart at abdominal segment 7/8. A second incision was made intersecting the first incision, going vertically following the aorta until reaching the head of the animal. A third incision was made horizontally at the end of the second incision to open the thoracic cavity. Four pairs of pins were placed at each border of the 1st thoracic segment, 1st abdominal segment, 5th abdominal segment and the 7th abdominal segment in order to open the thoracic and abdominal cavities by stretching the tissue (Fig. 3.1b).

Muscle characterization

Dissected tissue was stained using bromophenol blue diluted on Ringer's saline solution (5mg/ml for 3 minutes). After staining, muscles were described under a stereomicroscope by drawing their arrangement while removing muscles layers until reaching the cuticle. Additional stained tissue was mounted temporarily in microscope slides. These samples were observed under an AmScope T490B-DK microscope and photographed with a piece of metric paper (1mm grid) using a 108MP phone camera (Motoroloa Edge, 2021) attached to the ocular. A scale was added to the obtained images on ImageJ (National Institutes of Health; http://imagej.nih.gov/ij/) by transforming pixel units to the known length of the metric paper grid. These images were used to produce more detailed drawings using the GNU Image Manipulation Program (GIMP 2.10.10,

www.gimp.org). Each described muscle was named based on Bate (1993) and Landgraf et al. (1997), using the position and orientation of the muscles.

Nervous tissue characterization

After dissection, the stretched tissue was fixed with Bouins solution **(**Sigma) for 1 minute and washed three times with PBT solution [1x Phosphate-buffered Saline (PBS) and 0.1% Triton-X 100]. Guts and body fat were then carefully removed with tweezers and a bended pin head. After removing the pins, the tissue was washed and permeabilized in five PBT baths for an hour (12 min/bath).

Immunohistochemistry was used to visualize the neuronal tissue. We assessed the cross reactivity of antibodies designed against *D. melanogaster* proteins in the *Chironomus sp*. "Florida" tissue (Table 1). The conjugated antibody Cy3 goat anti-HRP (1:300; Jackson ImmunoResearch) and the following primary antibodies: mouse anti-Syn [1:20; Developmental Studies Hybridoma Bank (DSHB)], mouse anti-Dlg (1:20; DSHB), rabbit anti-Dlg (1:150), mouse anti-FAS2 (1:10; DSHB), mouse anti-α -Tubulin (1:3000; DSHB), mouse anti-BruchPilot (1:50; DSHB), mouse anti-Synaptotagmin (1:50; DSHB), mouse anti-Fustch (1:10; DSHB), mouse anti-GluRIIA (1:20; DSHB) and rabbit anti-GluRIII (1:2000), were tested. The immunohistochemistry process was initiated by incubating clean *Chironomus* tissue in a mix of primary antibody and PBT overnight at 4ºC. This incubation was followed by five PBT washes during 1hr (12min/wash) to remove the excess of free antibody. A second 1hr incubation of the tissue was pursued in the dark with a mix of PBT, the conjugated antibody and the respective secondary antibody [Alexa Fluor 488-conjugated AffiniPure goat anti-mouse or anti-rabbit IgG (1:300; Jackson

ImmunoResearch)]. A second wash of five changes of PBT in the dark was applied to remove the excess of secondary antibody. These tissues were mounted on glass microscope slides using Vectashield (Vector Labs) as mounting media. The preparations were sealed with nail polish and stored in a cool dark place until analysis.

The specimens were scanned using a Nikon Eclipse Ti inverted A1R laser scanning confocal microscope. NIS elements Advance Research 4.5 acquisition and analysis software was used for image acquisition. Complete body tissue recordings were obtained over the Z-axis (0.5 um depths) at 20X magnification. Recording of specific features such as ganglions and nerves were obtained at 40X (0.2 um depths) while the NMJs at 40X and 100X (0.2 and 0.1 um depths, respectively). Large structures were recorded by scanning multiple areas in the X or Y axis with an overlap of 20% of the scanned area. Images were made in Image J as Maximum Intensity Projections over the Z-axis of the stack of images. To better visualize some NMJ structures the background of the image was attenuated by using the GNU Image Manipulation Program. Briefly, the silhouette of the studied synaptic terminal was selected by hand on the color channel containing the HRP staining. The width of this selection was increased to 1 pixel size and later inverted to erase the area of no interest. The GNU Image Manipulation Program was also used to create diagrams from raw images to show the location and appearance of ganglions, nerves and NMJs. A nomenclature to these structures was assigned based on previous work by Miall and Hammond (1900), Bate (1993), and Landgraf et al. (1997).

Selection and characterization of a model NMJ

The selected NMJ model was observed in the tissue of 10 immunolabeled larvae with SYN and HRP. The number of boutons were quantified under an Eclipse 80i microscope at 60X**,** and recordings of the muscles were obtained using the confocal laser scanning microscope. The area of these muscles was determined on Image J by drawing a polygon on top of the muscle silhouette then using the measurement option to obtain the value. The density of boutons was determined by dividing the number of boutons by the respective muscle area. The average and the variability of density of boutons was determined.

Results

The associated musculature of the first abdominal segment

Three orientations of muscles (longitudinal, transverse, and oblique) can be distinguished in the ventral, lateral and dorsal area of the thoracic and abdominal region (Fig. 3.2). In the first abdominal segment, there are 31 muscles per hemisegment, being observed 12 lateral, 10 ventral and 9 dorsal muscles. Regarding the orientation of the muscles in the ventral and lateral area, we can observe 8 oblique, 9 longitudinal and 5 transverse muscles per hemisegment. Muscle fibers are present in two layers, presenting 3 main muscles in the internal part and 7 muscles in the external part of the ventral region. We defined a nomenclature based on position and orientation to label the muscles of the ventral and lateral region. Five groups of muscles were defined: Ventral external longitudinal (VEL), Ventral internal longitudinal (VIL), Ventral oblique (VO), Lateral

transverse (LT), and Lateral oblique (LO). For more details regarding the distribution of these muscles through the tissue refer to Fig. 3.4.

Antibody reactivity in the nervous tissue of *Chironomus* sp. "Florida"

From 10 tested antibodies, only six presented immunoreactivity (Table 3.1). With these reactive antibodies we were able to visualize neuron membranes, synaptic vesicles, microtubules, active zones and post-synaptic scaffold proteins. No antibody was able to enhance the visualization of glutamate receptors in the post-synaptic area of the muscle. The primary antibody mouse anti-Syn and the conjugated antibody Cy3 goat anti-HRP were used to study the neuromuscular system given their usefulness to describe qualitatively and quantitatively the tissue. Ganglion, nerves, axons, NMJs and the muscles were easily visualized with HRP. NMJ varicosities and synaptic boutons were easily visualized using Syn.

The central nervous system

The central nervous system of *Chironomus* sp. "Florida" is composed of a supraoesophageal and suboesophageal ganglia, three thoracic ganglia and eight abdominal ganglia (Fig. 3.3). The supra and suboesophageal ganglia are located out of the head in the prothorax and they are accompanied by the first thoracic ganglion. The second and third thoracic ganglia are in the mesothorax. The first abdominal ganglion is in the metathorax, leaving the first abdominal cavity unoccupied. Abdominal ganglia 2-6 occupy their respective abdominal segments. The 7th and 8th abdominal ganglia are both located in the 7th abdominal segment forming the terminal ganglion of the nerve cord.

Nerves move out from each ganglion to their respective region: nerves from the sub and supraoesophageal ganglia reach only the head, the ones from the thoracic ganglia reach the thorax, and the ones from the abdominal ganglia reach their respective abdominal segment. Each ganglion is composed of two lobes that are interconnected through a ventral nerve cord, a structure that is also doubled but appears as a single feature in almost all the body.

Nerves projecting to the first abdominal segment

There are two main nerves originating from the first abdominal ganglia: the transverse nerve and the main nerve. The transverse nerve innervates the segmental border muscle (SBM) while the main nerve separates in different tracts that reach different areas of the firs abdominal segment. There were six nerve tracts originating from the main nerve: *ventral nerve a, ventral nerve b, ventral nerve c, ventrolateral nerve, lateral nerve*, and *dorsal nerve*. As their name says, the terminals of each of these nerves tracts reaches muscles in specific areas of the hemisegment (Fig. 3.4).

The first abdominal segment NMJs

Motor neuron terminals or NMJs are distributed through all the tissue and present a great variability in sizes and bouton appearance (Fig. 3.5 and 3.6). It can be observed four NMJ sizes: large, medium, small, and very small (Fig. 3.5A-D). Large size NMJs are located in muscles VIL1-3 and VEL5 and show very small varicosities that do not produce quantifiable synaptic boutons (Fig. 5A and 6A). Medium size NMJs are located in muscles VEL2-4 and VEL6 and show very well distributed varicosities that form quantifiable synaptic boutons (Fig. 3.5B and 3.6B). Small size NMJs are located in muscles VIL1 and

LO1 showing small varicosities that do not produce quantifiable synaptic boutons (Fig 3.5C and 3.6C). Very small synapses are located in muscles VO1, LT1-4, and LO2-9 (Fig. 3.5 and 3.6D-F). Synaptic terminals in LT1-4 show a mix of tightly grouped and very distributed varicosities that produce quantifiable boutons of various sizes (Fig. 3.6D). Varicosities in VO1 and LO2-9 are very condensed, producing mainly unquantifiable boutons but sometimes quantifiable boutons are visible (Fig. 3.6E-F).

Selection and description of the model NMJ VEL2

The model NMJ was selected based on multiple criteria: 1) the NMJ is innervating an important muscle, 2) is easy to differentiate between other synapses, and 3) can be easily visualized. In addition, we considered the facts that 4) its size is not an obstacle for its study, and 5) synaptic boutons are easy to visualize and quantify.

The NMJ located on muscle VEL2, is a structure contained within a muscular area ranging from 22017 to 69982 μm^2 ($\bar{X}$: 44627; σ: 13452, n=19). This neuromuscular junction is a median size synaptic terminal that originates from the *ventral nerve a* tract and is located in the external ventral muscle layer of the first abdominal segment. Its typical structure has two main branches covered with varicosities or synaptic boutons, but secondary branches are also commonly observed. Its synaptic boutons are rounded, well distributed and cover a great part of the structure (Fig. 7). The number of synaptic boutons ranges between 47 to 140 ($\bar{X}$: 86.89; σ: 24.04, n=19) with densities of 0.0008 to 0.0046 boutons/ μm^2 ($\bar{X}$: 0.0022; σ: 0.0012, n=19).

Discussion

The main purpose of this work was to describe the neuromuscular system of *Chironomus* sp. “Florida”. This description was needed to provide new insights about the neuromuscular anatomy in the *Chironomus* group in order to identify potential structures to use as CTMs. It was of great interest to study specifically the NMJs, since works with *D. melanogaster* have highlighted the responsiveness of these structures to external factors (e.g., Hirsch et al., 2012; Sigrist et al., 2003; Zhong & Chun-Fang Wu, 2004). Although partially known, the *Chironomus* neuromuscular anatomy has always been incomplete. Miall and Hammond’s work on *Chironomus dorsalis* presented a general view of the system, only describing the first layers of muscles without naming and relating them to the nervous system (Miall and Hammond 1900). Nerve tracts and the NMJs were not described by this author nor by recent studies describing the nervous system in other *Chironomus* species (e.g., Robertson et al. 2014b, Richardi et al. 2015, Ospina-pérez et al. 2019). The description presented in this work fill all these gaps resulting in an anatomy full of interesting features that could be used for toxicologic studies.

The *Chironomus* larval abdominal muscular anatomy presented in this work is the most detailed available. It is unique when compared with the anatomy of other abdominal muscle arrangement described in other insect species such as in *D. melanogaster* (Bate 1993), *Periplaneta americana* (Shankland 1965), and *Galleria mellonella* (Randall 1968). Comparing the muscular anatomy of *Chironomus* with other insect anatomies is challenging since current insect descriptions uses different body sections to characterize the muscle distribution. In this study, we focused in describing the first abdominal segment since the abdominal region of the larval stage is the most used for movement. Similar

abdominal descriptions are common for the crawling larvae of insects [e.g., *D. melanogaster* (Landgraf et al. 1997)]. Nevertheless, studies describing the anatomy of adult winged insects typically examine the thoracic section of the body given its relation to movement [e.g., *Hemianax papuensis* (Simmons 1977)]. It is also true for the musculature descriptions of walking insects with well-developed appendages where the musculature descriptions of the thorax and appendages are preferred [e.g., *Locusta migratoria* (Hoyle 1954)].

When comparing the *Chironomus* anatomy to other crawling larvae such as *D. melanogaster,* we can notice that some muscle arrangements in the first abdominal segment are preserved while others are completely missing. This is the case for the *D. melanogaster* ventral acute and ventral transverse muscles, which are completely missing in our model while lateral transverse muscles with their segment border muscles are preserved almost identically. Another outstanding character of the *Chironomus* musculature is that there are multiple LO muscles compared to the single LO muscle structure seen in *D. melanogaster*. The same is observed with the VO muscles, but this time the *Chironomus* anatomy only shows a single VO muscle structure while *D. melanogaster* shows multiple. The number of muscles per hemisegment in the first abdominal segment of the studied *Chironomus* species is similar to the number of muscles in *D. melanogaster* (31/*Chironomus* hemisegment vs 30/ *D. melanogaster* hemisegment (Beckett and Baylies 2006) however, the muscles between both species are distributed inequitably through the ventral, lateral and dorsal regions.

The central nervous system in the *Chironomus* larva is known from other species (e.g., Miall and Hammond 1900, Richardi et al. 2015, Ospina-pérez et al. 2019) and the

description shown in this work is similar. The present peripheric nervous system description in contrast, shows new features such as the different nerve tracts originating from the main nerve and their multiple NMJs. Nerve tracts trajectories in *Chironomus* bear similarities to the trajectories of the nerve tracts observed in *D. melanogaster*. The *Chironomus* dorsal nerve trajectory appears to correspond to the *Drosophila* internal segmental nerve (ISN) trajectory, the *Chironomus* ventral a-c nerve trajectory to the *Drosophila* segmental nerves b-d (SNb-d) and the *Chironomus* lateral nerve trajectory to the *Drosophila* segmental nerve a (SNa). Nevertheless, tracing techniques such as retrograde labeling with different dyes needs to be performed in the future to corroborate the exact nerve trajectories in the abdominal segment of the *Chironomus* larvae. Pursuing this method should also allow the identification of the motor neurons cell body innervating the muscles (Inal et al. 2020).

Synaptic terminals in the *Chironomus* tissue show a large variability of sizes. This is just a reflection of the high variability in muscle size through the larval tissue. The great variability of synaptic varicosities made it difficult to identify suitable NMJs with quantifiable synaptic boutons. Similar variations in varicosities were observed by (Johansson et al. 1986) in *Chironomus tentans* when trying to detect bombesin neuroreactivity in nerve fibers of the alimentary canal of the larvae. The quantifiable structures in the ventral and lateral area can only be identified in the VEL muscles. These muscles present an assortment of rounded and well-formed synaptic bouton making their quantification easy under the microscope. NMJs on LT muscles also present quantifiable synaptic boutons, but their quantification is difficult due to the presence of large amounts of fat tissue on top of these terminals.

The model synapse (VEL2) was selected due to its visible location in the tissue and due to its quantifiable boutons. Compared to *D. melanogaster* model NMJ the *Chironomus* model NMJ is characterized by its larger size, separated bouton arrangement and simple structure with elongated branches. The large variability in the number of boutons can reflect several factors such as differences in larval size, sex, and age. Some of these factors are known to affect the structure and functioning of synaptic terminals in *D. melanogaster* (Lnenicka et al. 2006, Menon et al. 2013) thus similar effects could be occurring in the *Chironomus* NMJ. Future experiments will have to be undertaken to assess whether these factors play a role. If they are, it should be possible to reduce the *Chironomus* synaptic size variability by only considering a subset of animals.

Glutamate receptors (GluRs) are present in the postsynaptic side of the NMJs of insects (Usherwood 1994). Sadly, we were not able to detect the subunits of these structures in the muscles of *Chironomus* by using antibodies with reactivity in the *D. melanogaster* nervous tissue (see Table 1). We can still infer the presence of GluRs in the *Chironomus* tissue, but the subunits composing the *Chironomus* GluRs should be different from those identified in the *D. melanogaster* tissue. Future directions in the study of the postsynaptic region of the *Chironomus* NMJ should focus in identifying these receptors by the identification of their subunits. This could be achieved in part by pursuing a genome-wide identification, characterization, and classification of GluRs genes as pursued with other insect species (Wang et al. 2018).

Our study on the neuromuscular system of *Chironomus* provides the basis to identify features in the NMJ that could be used as markers for assessing toxicity. In addition to quantifying the number of boutons, the muscle area, and the density of boutons, other

features such as quantifying presynaptic area, synaptic arborization, active zones and postsynaptic area could be used if the adequate immunohistochemical techniques are worked out. Given the outstanding neuromuscular anatomy of *Chironomus*, procedures such as electrophysiology, a method that measures electrical activity at the NMJ, could also be used to determinate disruptions on neuronal signaling and synaptic transmission caused by toxic chemicals. Due to the versatility of this system, we encourage future studies to be done in order to evaluate the responsiveness of the NMJ to biological, environmental and toxicological variables.

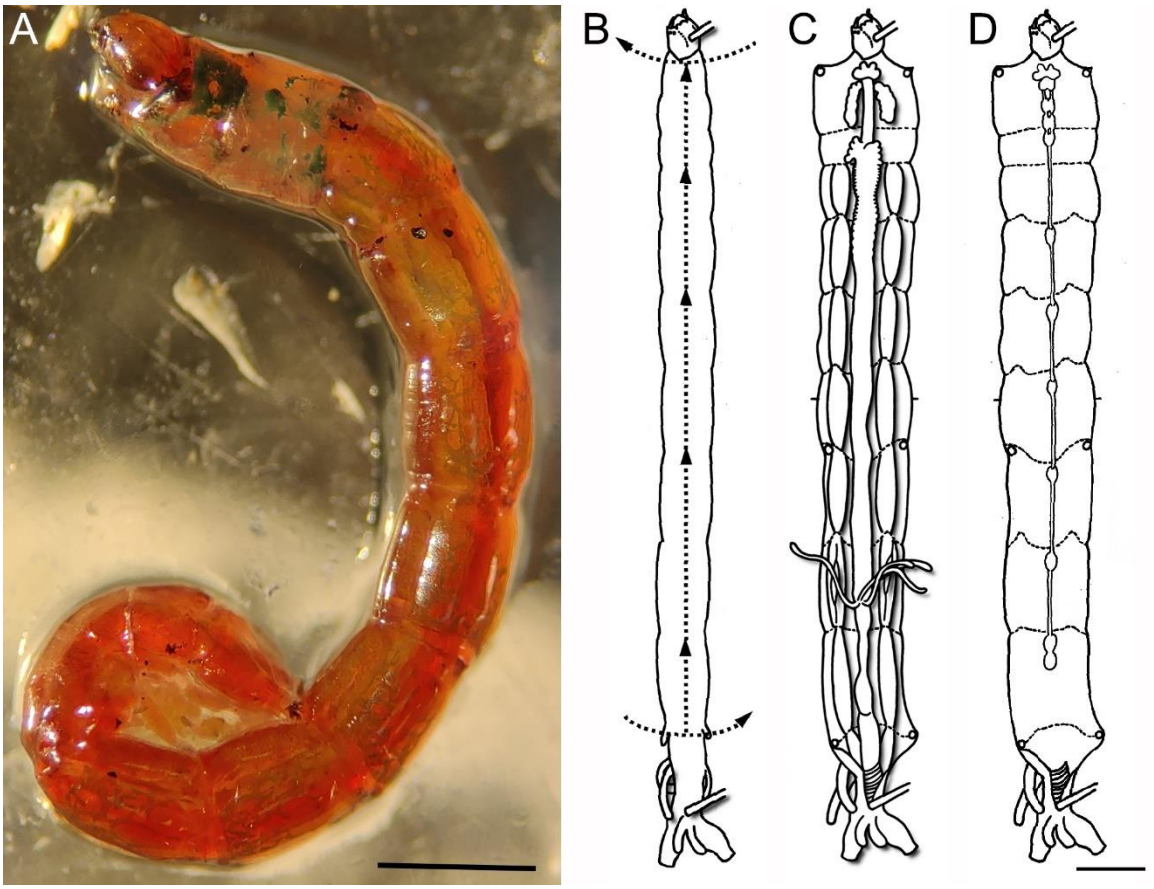

Figure 3.1. The fourth larval instar of *Chironomus* sp. Florida and the dissection technique used to obtain the neuromuscular tissue. A) The entire body of the 4th instar larvae is bright red with some green spots in the thorax in completely mature larvae. This stage is characterized by individuals having a length between 6-14mm. B) Schematic view of the dissection process adapted for studying the neuromuscular tissue of *Chironomus* sp. "Florida". From left to right: Initial position of larvae in the plate after pinning, larvae after stretching the tissue, and larvae after removing the visceral tissue and fat. Dash lines and arrows represents the dissection path guides. Scale: 1mm.

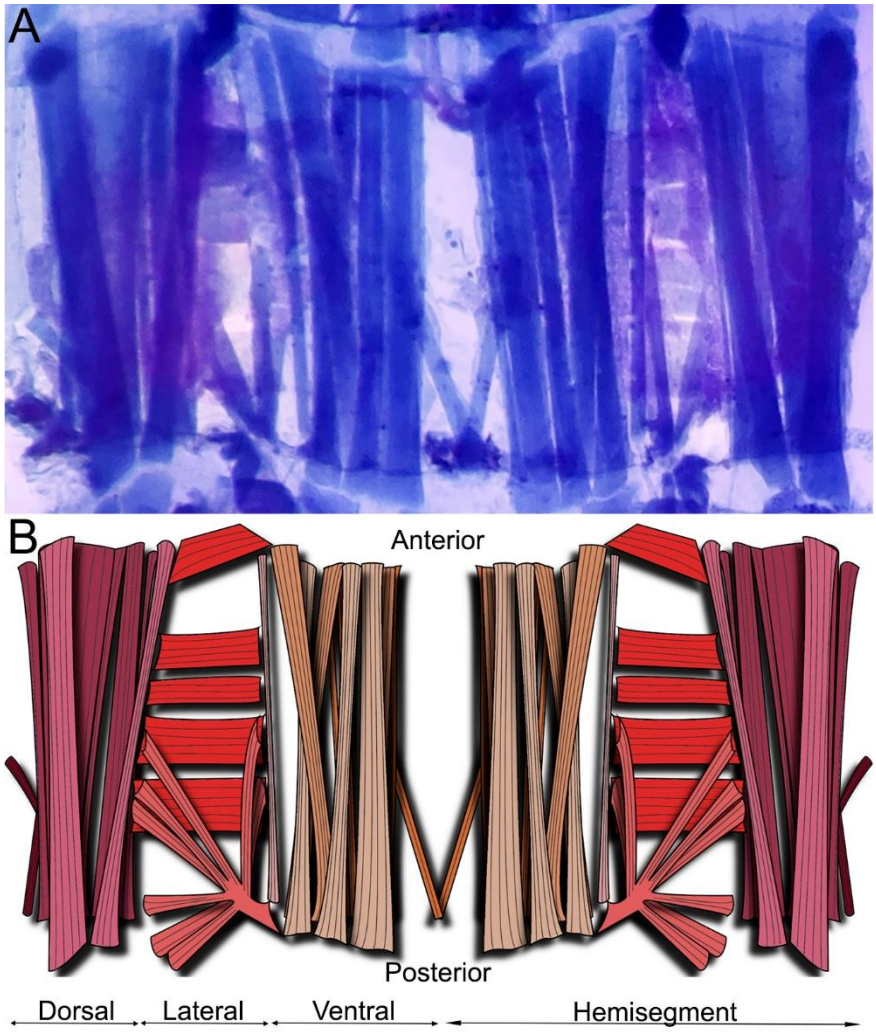

Figure 3.2: Musculature of the first abdominal segment of *Chironomus* sp. "Florida". A) First abdominal segment as observed with the bromophenol blue staining. B) Diagram showing the position and orientation of muscles in the first abdominal segment. Purple: dorsal muscles; Red: lateral muscles; Orange: ventral muscles. Light colors represent internal muscles while dark colors external muscles.

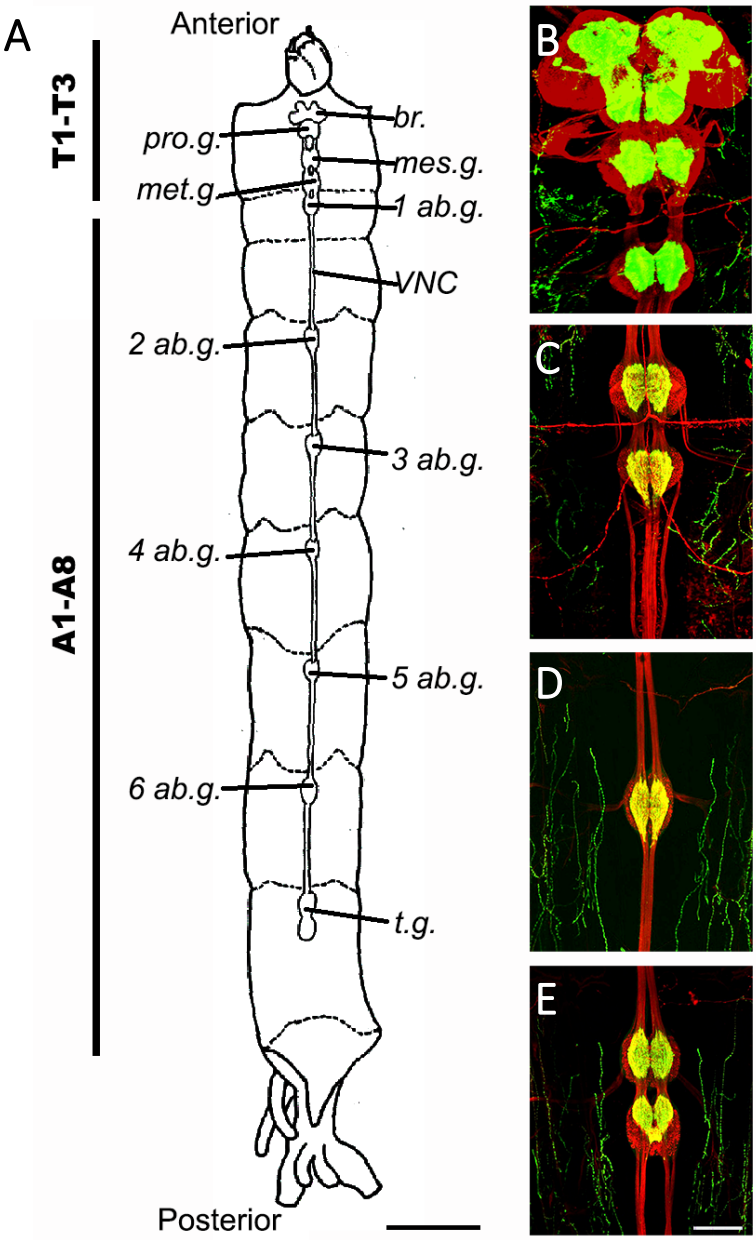

Figure 3.3: Principal components of the central nervous system of the larval *Chironomus* sp. "Florida". A) General view of the CNS with nomenclature of principal structures. Scale: 1mm. B) Representative view of the brain, prothoracic ganglion and mesothoracic ganglion. C) View of the metathoracic ganglion and the first abdominal ganglion. D) Representative view of an abdominal ganglion as observed with the 5th abdominal ganglion. E) View of terminal ganglia. Scale B-E: 100um.Visualization of neuronal walls and synaptic boutons are enhanced using HRP (red) and anti-Synapsin (green). Abbreviations: Tx. Thoracic segment x, Ax. Abdominal segment x, br. Brain, Pro.g. Prothoracic ganglion, Mes.g. Mesothoracic ganglion, met.g.: Metathoracic ganglion, ab.g. x. Abdominal ganglion x, t.g.. Terminal ganglion, VNC. Ventral nerve cord.

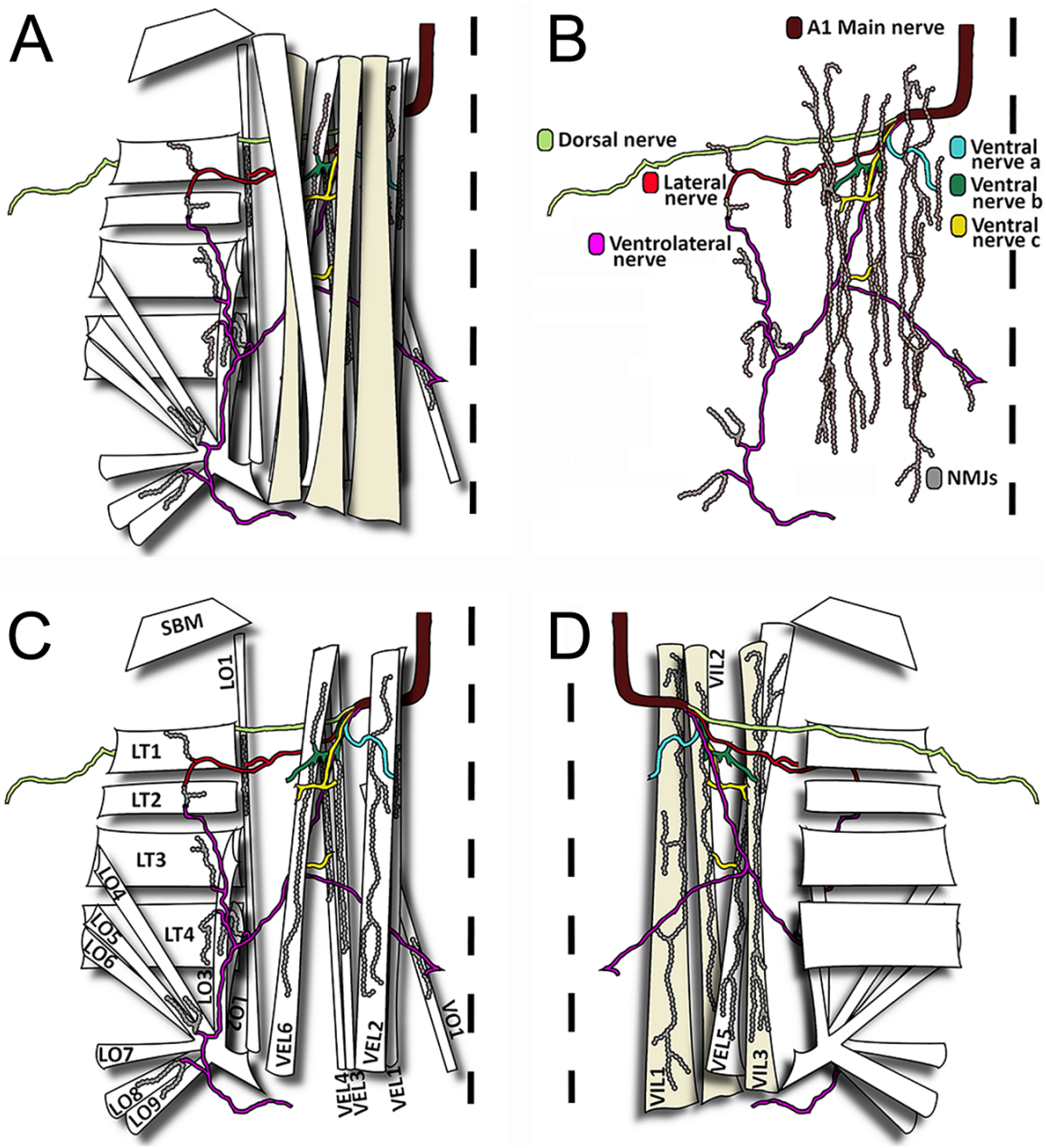

Figure 3.4: The neuromuscular network of the lateral and ventral area of the first abdominal segment. A) Schematic representation of body wall muscles of one hemisegment with their respective peripheral nerve branches and neuromuscular junctions. B) Network of NMJs with their respective nerves. C) View of the external layer of muscles as observed from the front. D) View of the internal layer of muscles as observed from behind to show the morphology of typical NMJs. Each nerve branch is represented with a single color to show target muscles. Muscle and nerve nomenclature based on Bate 1993 and Landgraf et al. 1997 as position, orientation, and number. Abbreviation: Position V: ventral; VI: Ventral internal; VE: Ventral external L: lateral. Orientation: L: longitudinal O: oblique; T: transverse, SBM, segment border muscle.

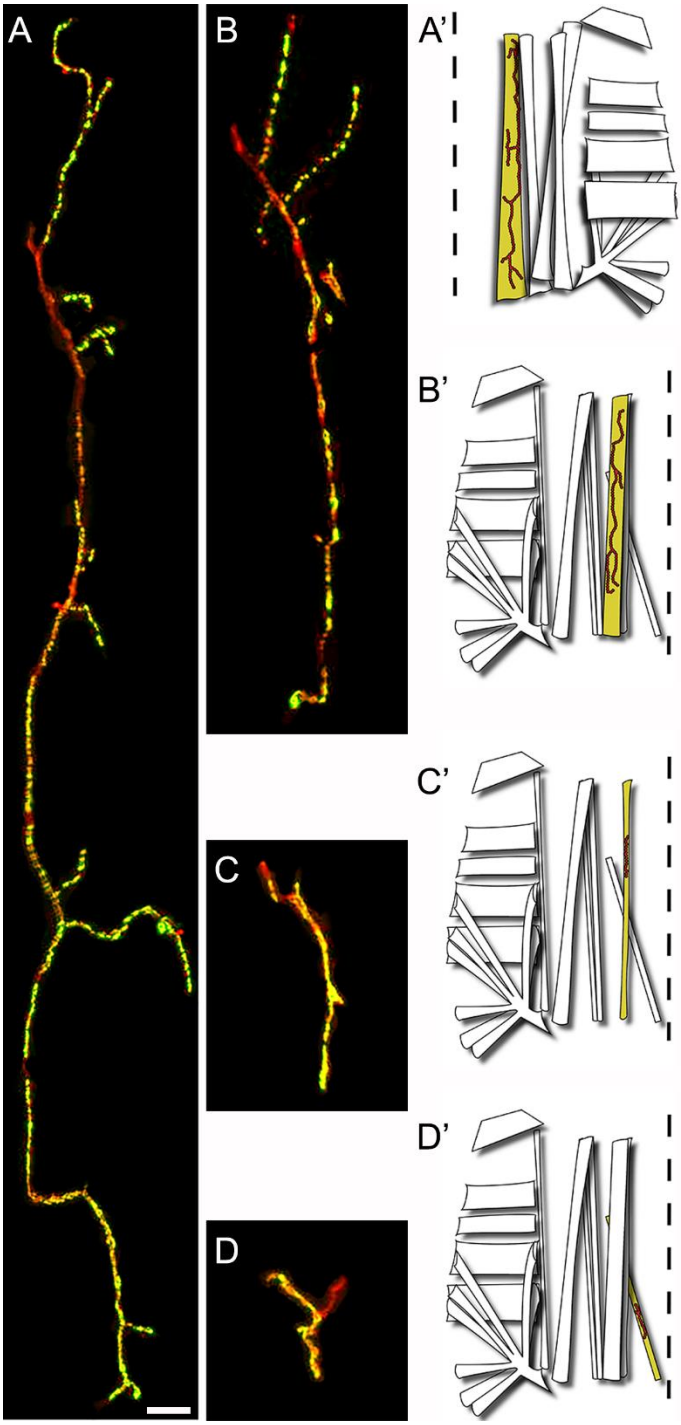

Figure 3.5: Size diversity of NMJs through the muscles in the first abdominal segment. A) Representation of a large ventral internal NMJ as observed in muscle VIL1. B) Representation of a medium ventral external NMJ as observed in muscle VEL2. C) Representation of a small NMJ as observed in LO1. D) Representation of a very small NMJ as observed in VO1. A'-D') Muscle location of the NMJs presented in A-D in order of appearance from top to bottom. Inmmunohistochemistry: HRP (red) and anti-Synapsin (green). Scale 100um (A-D).

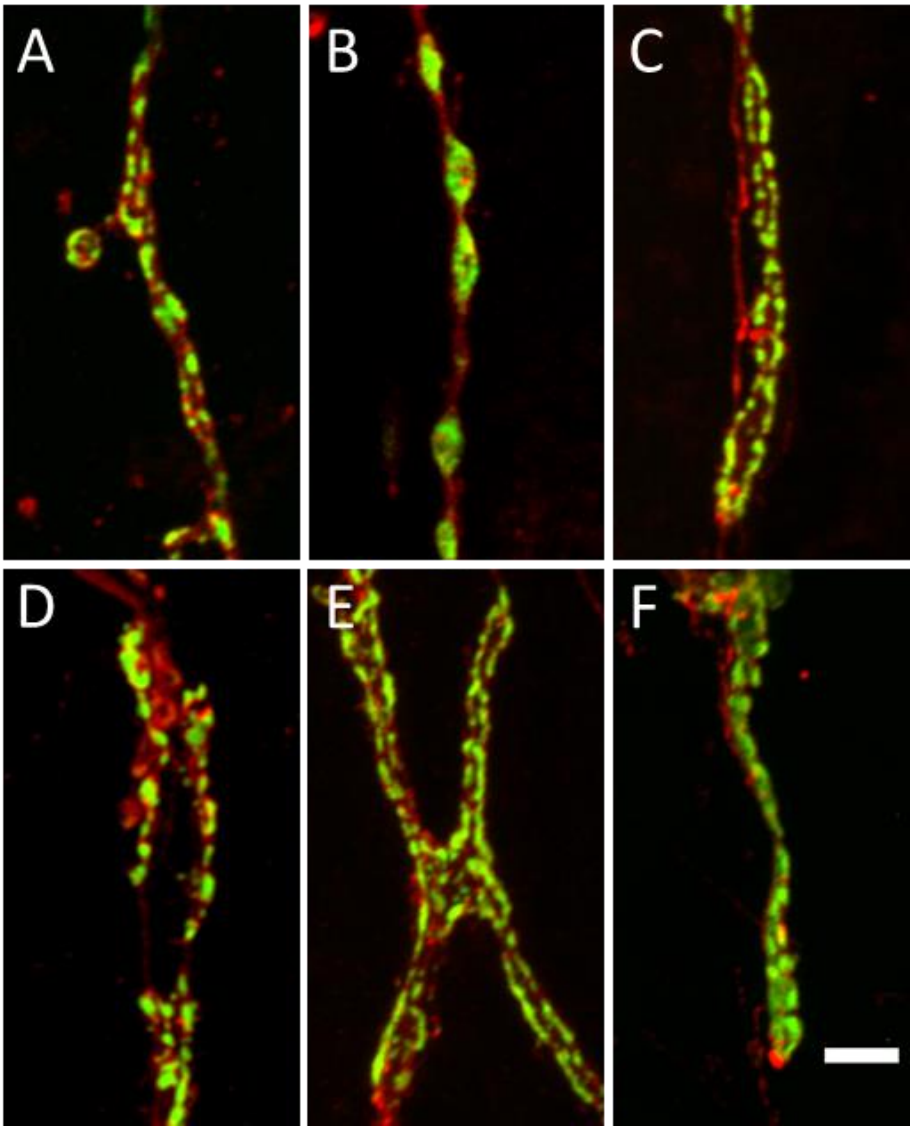

Figure 3.6. Varicosities observed through the NMJs of the first abdominal segment. A) View of a section of the VIL1NMJ showing the unquantifiable boutons commonly observed in large size synapses. B) View of a section of the VEL2NMJ showing the quantifiable boutons commonly observed in medium size synapses. C) View of a section of the LO1 NMJ showing the unquantifiable boutons commonly observed in small synapses. D) View of a section of the LT2 NMJ showing the characteristic quantifiable boutons of various sizes observed in the very small NMJ from LT muscles. E and F) View of a section of the LO4-6 NMJs showing the unquantifiable (E) and quantifiable (F) boutons that show independently through these very small NMJs. Immunohistochemistry: HRP (red) and anti-Synapsin (green). Scale 5 um.

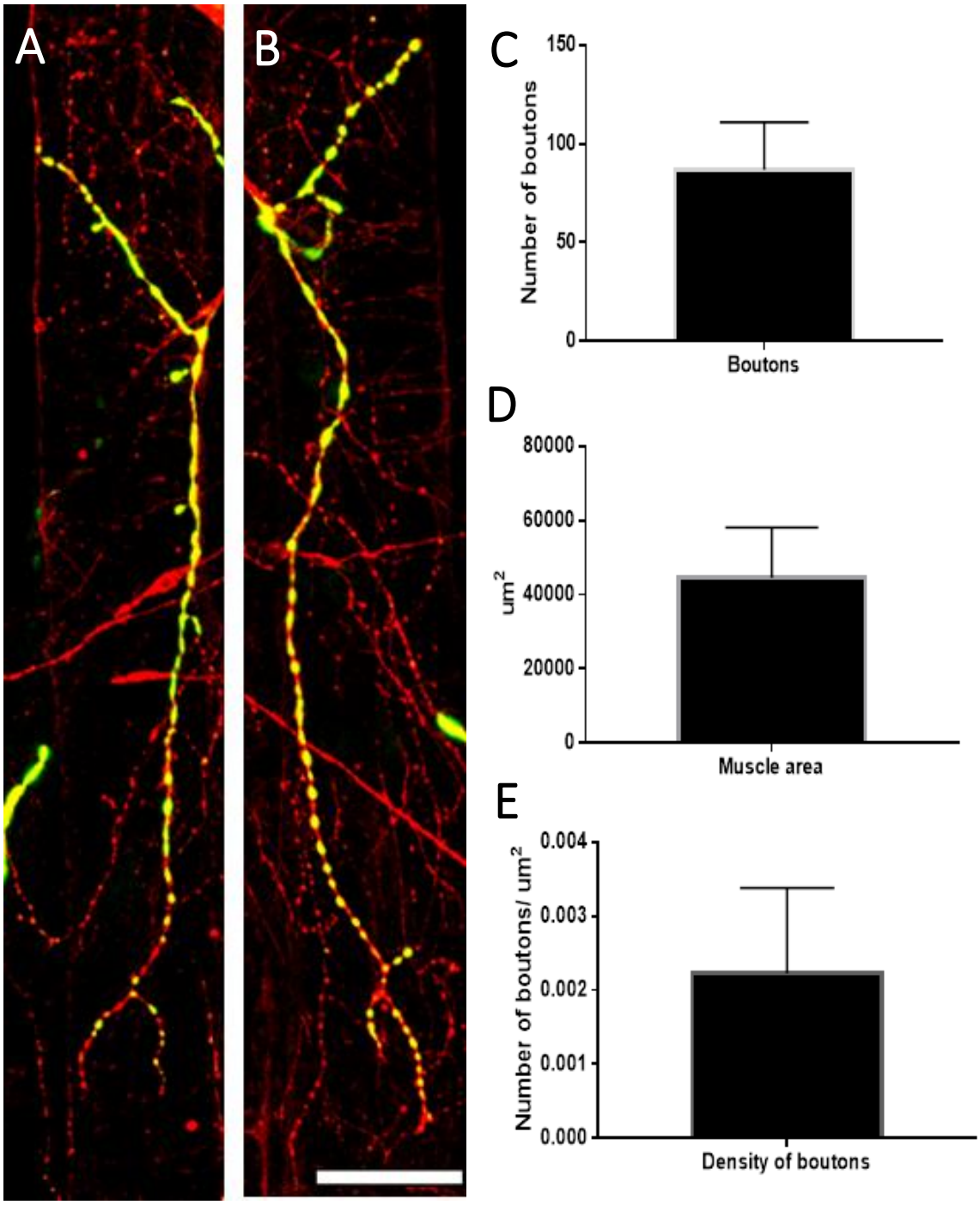

Figure 3.7: Confocal views of the model NMJ (VEL2) with mean values of the three quantified cellular markers. A) Right and B) left VEL2 NMJs obtained from the tissue of a single larvae. C-E) Average number of boutons, muscle area and density of boutons acquired from the study of 19 VEL2 NMJ obtained from 10 dissected larvae. Error bar represents the standard deviation of the data. Immunohistochemistry: HRP (red) and anti-Synapsin (green). Scale 50um.

Table 3.1: Antibodies with reactivity in the tissue of *Chironomus* sp. “Florida”.

Tested antibody	**Target**	**Immunoreactivity**
Anti-HRP	Presynaptic membrane	Yes
Anti-FAS2	Presynaptic membrane	Yes
Anti-α -Tubulin	Microtubules	Yes
Anti-Synapsin	Presynaptic synaptic vesicles	Yes
Anti-BruchPilot	Presynaptic active zones	Yes
Anti-DLG2	Post synaptic scaffold proteins	Yes
Anti-GluRIII	Post synaptic glutamate receptors	No
Anti-GluR2A	Post synaptic glutamate receptors	No
Anti-Synaptotagmin	Presynaptic vesicles	No
Anti-Fustch	Microtubule associated protein (MAP1B)	No

CHAPTER 4

RESPONSE OF CELLULAR MARKERS DERIVED FORM THE NEUROMUSCULAR JUNCTION OF *CHIRONOMUS* SP. "FLORIDA" TO ENVIRONMENTAL, BIOLOGICAL AND CHEMICAL FACTORS.

Introduction

Chironomids are a group of insects that play an important role in stream ecosystems. Their larvae are ubiquitous and present a wide range of feeding behaviors, ranging from grazers and leave miners to filter feeders and detritivores (Armitage et al. 1995). Some species of chironomids are sediment dwellers, helping in the movement of nutrients from the sediment to the water column (Gautreau et al. 2020). They also have the capacity of enhancing benthic aerobic respiration due to their movement behavior in the sediment (Baranov et al. 2016). This relation with sediments makes chironomids prone to be in contact with contaminants, thus bioaccumulating and moving them through the food web in and out stream ecosystems (Runck 2007). Although chironomids are tolerant to many contaminants, they shown an array of responses at molecular and morphological level (Warwick et al. 1987, Kuhlmann et al. 2000, Lee et al. 2006). These responses have been used by many authors to assess water and sediment toxicity. Their response to contaminants and their ecological role, short life cycles, and versatility under laboratory conditions make of these insects an excellent model organism for assessing toxicity in freshwater ecosystems (Ingersoll et al., 2000).

Chironomus sp. "Florida" is a neotropical species that plays an ecologically relevant role in aquatic environments in Puerto Rico. This chironomid has not been used

as model organism for assessing toxicity, but its extremely short larval development (7-14 days) (Reyes-Maldonado et al. 2021) makes it an excellent candidate. The neuromuscular tissue of this animal has been described and the neuromuscular junction (NMJ) has been highlighted as a promising cellular and tissue marker (CTM) (Chapter 3). The NMJ is a highly specialized synapse between a motor neuron nerve terminal and its muscle fiber, which is the cause of movement in the animals (Rodríguez Cruz et al. 2020). The presynaptic terminal of the NMJ is packed with varicosities called synaptic boutons, small protuberances filled with synaptic vesicles containing the neurotransmitter (Collins and DiAntonio 2007). These structures are responsive to several environmental, biological, and neurotoxic factors (e.g., Hirsch et al., 2012; Sigrist et al., 2003; Zhong & Chun-Fang Wu, 2004) resulting in a promising CTM for assessing toxicity with chironomids. As new pollutants arise in stream ecosystem due to urban development, it is imperative to elaborate biological tools to assess the impact of emerging and toxic compounds in the ecosystem.

New pollutants, such as phthalates and extremely toxic heavy metals, are of great concern due to their appearance in aquatic ecosystem. In Puerto Rico phthalates have been found in freshwater ecosystems (Ortiz-Colón et al. 2016) and water treatment plants (Soler-Llavina and Ortiz-Zayas 2017). Of all phthalates, the low molecular weight dibutyl phthalate (DBP) is one of the most common variants found at the highest concentrations in freshwater environments of the island (Ortiz Lugo and Sosa Lloréns 2015, Ortiz-Colón et al. 2016, Torres et al. 2018). DBP has been considered an endocrine disruptor with possible effects on the nervous system (Tseng et al. 2013) and decreased locomotion (Crooke Rosado et al. 2015), oxidative stress (Lu et al. 2017), and gene expression of stress related proteins (He et al. 2022) are some of the known effects of this chemical on aquatic fauna.

Heavy metals such as lead (Pb^{2+}) are of great concern in stream ecosystems given their ability to bioaccumulate on the tissue of animals and produce neurotoxic effects (Sanders et al. 2009, Lee et al. 2019). In Puerto Rico, reported Pb^{2+} levels in superficial sediment of some urban streams are low (Buttermore 2011) and much higher in estuarine areas (Webb and Gomez-Gomez 1998). The presence of these contaminants in aquatic ecosystems have been related to reduced survivability, changes in development and disruption of the nervous function on aquatic animals (Grosell et al. 2006, Kim and Kang 2017, Green and Planchart 2018).

Evaluating the effects of these compounds on the NMJ of the native species *Chironomus* sp. "Florida" could demonstrate how these emerging contaminants affect the nervous system of this animal. It also could provide us with an additional tool to assess stream toxicity. For these reasons the aim of this study was to assess the response of the *Chironomus* NMJ to toxic sediments spiked with DBP and lead. Given the toxicity of these chemicals on aquatic fauna, we expected to observe induced changes on the density of boutons related to the NMJ. These changes are expected to occur by disruptions in the natural distribution of synaptic boutons through the containing muscle area by the contaminants. To assess this, we have exposed the larvae of *Chironomus* sp. "Florida" to DBP and Pb^{2+}. High exposure concentrations were used to better analyze the toxic mechanisms of the compounds in the NMJ. Since biological and environmental variables such as larval age, sex, substrate media, temperature and oxygenation are known to affect the body morphology, molecular and cellular mechanisms, and the nervous system of insects (Williams et al., 1986; Maier et al., 1990; Bird, 1997; Sigrist et al., 2003; Zhong and Chun-Fang Wu, 2004; Lee et al., 2006; Lnenicka et al., 2006; Martínez-Guitarte et al.,

2007; Goedkoop and Spann, 2010), we first analyzed the response of the *Chironomus sp. "Florida"* NMJ components (number of boutons, muscle area and density of boutons) to these variables to discard any cofounding factor when assessing toxicity.

Materials and methods

Model Organism

The model organism used in our experiment was *Chironomus* sp. "Florida", a chironomid species that can be found inhabiting natural and artificial temporary pools in Puerto Rico. This species was first known from specimens collected in the southeast region of United States (Epler personal notification), but the complete geographical distribution of the species is unknow. Given the actual records of the species, we can infer that this insect possibly inhabits other Caribbean islands such as Cuba and Dominican Republic. This organism is easily differentiated from other *Chironomus* species because the larva has multi-toothed premandibles rather than premandibles with only two apical teeth like most *Chironomus* species (Epler, 2001). This chironomid is a fast-growing insect that can be easily cultured under laboratory conditions (Chapter 2). It represents an excellent option for studying the effects of contaminants over exotic aquatic models in Puerto Rico and the Caribbean since using native model have greater ecological relevance than exotic chironomid models. The larvae used in these experiments were obtained from laboratory reared colonies at the Institute of Neurobiology, University of Puerto Rico. These colonies were maintained following the methodology presented by Reyes-Maldonado et al. (2021). Recently laid egg masses were collected from these cultures prior the beginning of each experiment and 5 egg masses were assigned to each treatment. Egg masses were hatched

prior use by placing them in a covered petri dish with water at 25 or 30ºC according to the assay temperature during 24hrs. The resulted larvae were fed with few drops of a concentrated Tetramin suspension and used for the assays after 24hrs of hatching.

Sediment collection and characterization

Natural stream sediments were used to expose the larvae to the respective compounds. These sediments were collected from Quebrada Prieta (18°19'22.0"N 65°48'01.3"W, El Verde, Rio Grande), a first order stream located in a forested area. Particles with a diameter under 2mm were collected by scraping the first 3cm layer of the stream substrate with a stainless-steel spatula. Collected sediments were stored and transported to the laboratory at 4ºC in 4L glass jars. In the laboratory, sediments were placed in a stainless-steel container and homogenized by hand for 10 minutes using a paint/mud mixer. Before use, the organic content, particle size distribution and wet/dry ratio was determined. Organic content was assessed by determining the difference in weigh of a small sample after ignition at 500ºC for an hour; particle distribution was determined by sieving through a series of sieves for fractions above 0.5 mm; and the wet/dry ratio was obtained by determining the difference in weight of a small sample after drying at 50ºC during 24hrs. The homogenized sediment was distributed on a tray, divided in squares, and placed in an oven at 50ºC until dry. Later, the sediment squares were separated and kept staked in a covered glass container.

Sediment spiking

Two chemicals were used to spike the sediments: dibutyl phthalate (DBP) and lead chloride ($PbCl_2$) as source of Pb^{2+}. The spiking process was started by following a

methodology based on Bartsch et al. (1997), Borgmann and Norwood (1999) and Call et al. (2001b). Three sets of spiked sediments were produced for each compound at nominal concentrations of 0, 1000 and 1500ppm for DBP and 0, 500 and 5500ppm for Pb^{2+}. These high doses were selected based on the literature. A stock solution per concentration was prepared by dissolving the required DBP volume into 4 ml of acetone and the required $PbCl_2$ weight into 100ml of water. Each stock solution was spiked individually to 100g of pre-dried sediment. Each spiked sediment batch was homogenized by hand and the wet sediment [200g of dry weight (D/W) equivalent] was added to reach a total weight of 300g D/W of sediment. Deionized water equal to the volume lost in drying the 100g of sediment was added. At the end of the process, each container was covered and placed in a rolling mill during 24hrs to maximize homogenization between sediments and the compound.

Immunohistochemistry

Neuromuscular tissue of all treated larvae was obtained by following dissection techniques presented on Chapter 3. Neuromuscular junctions (NMJs) on muscles ventral-external longitudinal 2 (VEL2) from the larval first abdominal segment were immunolabeled using the conjugated antibody Cy3™ Goat Anti-Horseradish Peroxidase (HRP) and the primary antibody Mouse anti-Synapsin (Syn). Briefly, the clean neuromuscular tissue was incubated in a mix of primary antibody and phosphate buffered saline with 0.1% Triton (PBT) overnight at 4ºC (antibody concentration: 1/20), then five PBT washes were pursued during 1hr (12min/wash) to remove the excess of free antibody. A second 1hr incubation of the tissue was pursued with a mix of PBT, Alexa Fluor 488 goat anti-mouse and HRP (1/300 concentration each) followed by five PBT baths, both

processes executed at dark. The resulted tissues were mounted on glass microscope slides using Vectashield, sealed with nail polish and stored in a cool dark place.

Synaptic bouton and muscle area quantification

Synaptic boutons were quantified under an Eclipse 80i microscope at 60X magnification on the NMJs of both VEL2 muscles located on the first abdominal segment. Only rounded varicosities observed with the SYN staining were quantified. The area of the muscles was measured using the draw function on the red channel of NIS elements Advance Research 4.5 acquisition and analysis software on live images generated on a Nikon Eclipse Ti inverted A1R laser scanning confocal microscope at 20X magnification. Density of boutons was determined by dividing the number of boutons with the area of muscles.

Evaluating the effects of solvents, substrate, and other environmental and biological variables

Before starting the spiked sediment assays, we evaluated the effects of various variables on larval NMJ. We evaluated four substrate conditions to determine if the sediment or the acetone affected the number of synaptic boutons on the larval NMJ. The conditions were no sediment, shredded paper, sediment, and sediment spiked with acetone. The sediment and the sediment with acetone treatments were prepared using the same methods from the spiked sediment toxicity test but without adding the DBP and $PbCl_2$. The shredded paper substrate was obtained by shredding a generous amount of white coffee filter paper in distilled water until obtaining a paste. Each condition had three 400ml beakers replicas, which were filled with 2cm of substrate except for the no sediment

condition. Beakers were filled with water, placed randomly in a water bath, acclimated during 24hrs with constant aeration and supplied with 10 larvae. Treatments were maintained with constant aeration, a photoperiod of 12:12 light/dark and at 25±1ºC. During the assay, all larvae were fed daily at 2mg/larvae and 40% of the exposure water was changed with new acclimated water. When the larvae reached their 4th instar, they were randomly collected between replicas and immunolabeled for synaptic bouton, muscle area and density of boutons quantification.

Four environmental and biological variables (temperature, oxygenation, sex, and 4th instar larval age) were evaluated to determine if different conditions affected the number of synaptic boutons, the muscle area or the density of boutons on the larval NMJ. Temperature, sex, and 4th instar larval age were evaluated in conjunction by exposing larvae to 25 and 30ºC chronically. The following larval categories were studied at the end of the assay: early 4th instar females, late 4th instar females, early 4th instar males and late 4th instar males. Each temperature condition had 5 replicas, where 10 larvae were reared in 50ml falcon tubes provided with 40ml of water, 2cm of shredded coffee filter, constant aeration, and a photoperiod of 12:12 light/dark. When the larvae reached their 4th instar they were randomly collected through the replicas. Since all larvae categories had different developmental times, each category was collected for tissue preparation at its day of appearance. The 4th instar larval age was initially identified by the size and coloration of the individuals and later confirmed by observing the presence of respiratory organs inside the thorax. The larval sex was initially determined by the size of the larvae and later by observing the gonads inside the 7th abdominal segment.

Oxygenation was evaluated by exposing the larvae to conditions of hyperoxia, normoxia and anoxia. The hyperoxic treatments were prepared by adding constant aeration to 50ml falcon tubes, normoxic treatments by letting the falcon tubes uncapped without adding aeration and the anoxic treatments by capping the falcon tubes without leaving air space. Each condition had 5 replicas provided with 10 larvae, water, 2cm of shredded coffee filter, and a photoperiod of 12:12 light/dark. When the larvae reached their 4th instar they were collected randomly through the replicas.

During the duration of all assays, the tubes were maintained in a water bath regulated at ±1ºC of their target temperature, larvae fed daily at 2mg/larvae and 40% of the exposure water changed daily with the respective acclimated water. All collected larvae were immunolabeled for synaptic bouton, muscle area and density of boutons quantification.

Evaluating the effects of DBP and Pb^{2+} spiked sediment toxicity

The following treatments of spiked sediments were evaluated $DBP_{Control}$, DBP_{1000}, DBP_{1500}, $Pb^{2+}{}_{control}$, $Pb^{2+}{}_{500}$ and $Pb^{2+}{}_{5500}$. Each spiked sediment batch was divided into three replicas by adding 100g D/W of spiked sediment equivalent to three 400ml beaker. Beakers were filled with 300 ml of water and aerated during 24 hours before starting the exposure assay. For each chemical treatment, beakers (e.g., replicates) were placed randomly in a tray with water to maintain a temperature of 25±1ºC. 10 larvae were added to each beaker randomly. During the duration of the test, all treatments were maintained with aeration, at 25±1ºC, and with a photoperiod of 12:12 light/dark. When the larvae reached 4th instar, they were randomly collected through replicas and immunolabeled to quantify the number of synaptic boutons, muscle area, and density of synaptic boutons.

Each day pH, conductivity, temperature, and NH_3 were measured in all treatments and replicates. Alkalinity and hardness were measured on days 0, 1, 2 and at the end of the assay. Conductivity, pH, and temperature were measured using an Oakton PCSTestr 35 multiparameter. Alkalinity, hardness, and Ammonium were measured using a Hack test kit for alkalinity, and MColortest kits for Carbonate hardness and Ammonium test. Ammonium was measured by error and the results were transformed to Ammonia concentrations using the transformation provided by the Hach company:

$$[NH_3] = [NH_4]/0.9441$$

Statistical analysis

Differences between the number of synaptic boutons, muscle area and density of synaptic boutons and each assay treatments were determined using T test when comparing two treatments and one-way ANOVA followed by a post-hoc pairwise comparison Tukey's when comparing multiple treatments. For those groups of data that did not follow normal distribution a Mann Whitney test was pursued instead of a T test and a Kruskal-Wallis nonparametric test was applied followed by a Dunn's multiple comparison test instead of a one-way ANOVA. All data was processed on the statistical software GraphPad Prism version 7.00 for Windows (GraphPad Software, La Jolla California USA, www.graphpad.com).

Results

Physical characteristics of sediment

Natural stream sediment was mainly composed of sandy particles being 4.35% very fine gravel, 31.87% very coarse sand, 23.37% coarse sand, 28.70% fine to very fine sand, and 11.72% silt and clays. Organic matter and water content in the collected sediment represented the 8.37% and 33.03% of the total dry weight respectively (Table 4.1).

Variables inducing changes in the NMJ complex

The most important variables inducing changes in the number of boutons, muscle area, and density of boutons were the larval sex, temperature, oxygenation, and solvent presence (Table 4.2). Larval sex was observed to induce significant changes between the number of boutons and the muscle area of females and males reared at 25ºC and 30ºC (Fig. 4.1). Females in these conditions had higher number of boutons and higher muscle area than males. Nevertheless, significant induced changes in the density of boutons were only observed between males and females reared at 30ºC but not at 25ºC. In this case, males had higher density of boutons than females. The rearing temperature induced significant changes in the number of boutons and density of boutons when comparing same sex larvae reared at 25 and 30ºC (Fig. 4.2). At 30ºC both variables shown an increase when compared to the larvae reared at 25ºC. No effect was observed in the muscle area between both rearing temperatures. Higher larval mobility (breathing undulations) was observed in treatments exposed to 30ºC.

Oxygenation treatments induced significant changes by producing larvae with higher muscle area and lower density of boutons in hyperoxic conditions when compared

with larvae reared in normoxia (Fig. 4.3). No effect was observed with the number of boutons under these conditions. The effect of anoxia was not determined since larvae reared under this treatment died before reaching their 4th instar. Higher larval mobility (breathing undulations) was observed in treatments where larvae were exposed to normoxia. The sediment media with acetone did not induce any significant effects on the density of boutons when compared to the sediment media alone. Nevertheless, it was observed that larvae reared in the sediment with acetone had lower number of boutons and muscle area than larvae reared with only the natural sediment. No difference in the bouton number, muscle area and density of boutons was observed between larvae reared in sediment and the no substrate treatments.

DBP induce changes in the NMJ complex

During the DBP exposure test, pH was maintained similar and with little variability through all treatments ($DBP_{Control}$: 7.20 ± 0.10; DBP_{1000}: 7.30 ± 0.07; DBP_{1500}: 7.30 ± 0.07). Conductivity was variable through time and between treatments ($DBP_{Control}$: 217 ± 6.87; DBP_{1000}: 337 ± 188; DBP_{1500}: 230 ± 13.01) and was observed to increase when the sediment was suspended in the water column. NH_3 levels were maintained within known chironomid tolerable concentrations and were observed to increase through time mainly in the control, but slightly in the sediments containing DBP ($DBP_{Control}$: 0.4 ± 0.13; DBP_{1000}: 0.2 ± 0.07; DBP_{1500}: 0.2 ± 0.06). Hardness ($DBP_{Control}$: 97 ± 3.84; DBP_{1000}: 103 ± 3.84; DBP_{1500}: 103 ± 1.76) and Alkalinity measurements ($DBP_{Control}$: 92 ± 2.89; DBP_{1000}: 90; DBP_{1500}: 88 ± 2.89) tended to decrease while increasing the nominal concentrations of DBP

(Table 4.3). Water aeration and water temperature were maintained constant through time and treatments.

In the DBP toxicity test, larvae were ready for tissue analysis at the 4th day of exposure, where almost all larvae reached the 4th stage. Larvae presented significant DBP induced changes in the number and density of boutons, but not in the muscle area when comparing the $DBP_{Control}$ with the DBP_{1500} treatment (Table 4.5). Under these circumstances, the number and the density of boutons increased significantly in the presence of a high dose of DBP (Fig. 4.5). When comparing the $DBP_{Control}$ and the DBP_{1000} treatments there was not any statistical difference between the analyzed variables. When comparing treatment DBP_{1000} and DBP_{1500} density of boutons was the only variable that increased significantly in the higher dose.

Lead presence induce changes in the NMJ complex

In general, pH was maintained neutral during the Pb^{2+} exposure test ($Pb^{2+}_{control}$: 7.5 ± 0.10; Pb^{2+}_{500}: 7.4 ± 0.06; Pb^{2+}_{5500}: 7.1 ± 0.06). Conductivity increased by increasing the nominal concentration of lead in treatments ($Pb^{2+}_{control}$: 289 ± 3.88; Pb^{2+}_{500}: 329 ± 4.30; Pb^{2+}_{5500}: $_{5500}$: 908 ± 34.41). NH_3 was maintained under chironomids tolerable levels ($Pb^{2+}_{control}$: 1.25 ± 0; Pb^{2+}_{500}: 1.09 ± 0; Pb^{2+}_{5500}: 0.35 ± 0.04) but it was shown to increase through time. This increase was reduced in those treatments with higher lead in sediment. Hardness ($Pb^{2+}_{control}$: 130 ± 4.66; Pb^{2+}_{500}: 128 ± 5.36; Pb^{2+}_{5500}: 89 ± 7.94) and alkalinity ($Pb^{2+}_{control}$: 115; Pb^{2+}_{500}: 102 ± 2.89; Pb^{2+}_{5500}: 80) continued similar through time but decreased by increasing lead concentration (Table 4.3). Water aeration and water temperature were maintained constant through time and treatments.

The Pb^{2+} toxicity test lasted four days for treatments $Pb^{2+}_{Control}$ and $Pb^{2+}_{500,}$ and five days for treatment Pb^{2+}_{5500}. In this last treatment, larvae were underdeveloped, and had not reached the 4th instar for tissue collection at day 4th. The number of boutons was not affected in any of the treatments (Table 4.5). Changes in muscle area were observed to be induced significantly in treatment Pb^{2+}_{5500}, where a decrease in muscle area was observed when compared to the $Pb^{2+}_{Control}$ and Pb^{2+}_{500} treatment (Fig. 4.5). Bouton density increased significantly in both Pb^{2+} treatments when compared to the $Pb^{2+}_{Control}$. Pb^{2+}_{500} and Pb^{2+}_{5500} bouton density values were not significantly different when analyzing this variable.

Discussion

Here, we have explored how several environmental and biological variables, and toxicity conditions affects the NMJ of *Chironomus* sp. "Florida". Major findings indicate that larval sex, temperature, and oxygenation play an important role inducing changes in the VEL2 NMJ. Although the effects of DBP and Pb^{2+} have been addressed in other *Chironomus* species (Brown et al. 1996, Call et al. 2001a, 2001b, Martinez et al. 2001, 2004, Grosell et al. 2006, Arambourou et al. 2013), the response of the NMJ as a cellular marker to those compounds is innovative in this group. Given the known toxic effects of DBP and Pb^{2+} in aquatic fauna, we have anticipated their influence in the *Chironomus* sp. "Florida" neuromuscular tissue due to their ability in affecting locomotion, gene expression and survivorship in various invertebrate species (Spehar et al. 1978, Crooke Rosado et al. 2015, He et al. 2022).

Environmental and biological variables

The NMJ morphology is known to be affected by natural factors coming from the environment and the biology of the animals, such as temperature (Sigrist et al. 2003, Zhong and Chun-Fang Wu 2004), food deprivation (Stocker et al. 2018), gene variations (Campbell & Ganetzky, 2013), hyperexcitability (Budnik et al. 1990, Sigrist et al. 2003), and larval age and size variations (Menon et al. 2013). We only tested factors that were observed to be most relevant to our model organism. In our study, all the studied variables, except larval 4th instar age, affected either the number of boutons, muscle area or the density of boutons.

Larval sex has an important effect due to the sexual dimorphism presented by the studied species. Larval females are larger than males, often by as much as 2mm in length (Reyes-Maldonado et al. 2021). Larger size implies larger muscles with more synaptic boutons covering the muscle area (Menon et al. 2013). Determining the density of boutons solves for this discrepancy in size between females and males and should be used to remove the effect of larval size on the NMJ complex since no effect between sexes is observed after calculating it.

Temperature affected the number of boutons in our model, an effect that could be attributed to changes in larval behavior. At higher temperatures, larvae were observed to produce breathing undulations in a higher frequency than those exposed to lower temperatures, which barely exhibited this behavior. The increment in muscle activity by constant stretch and contraction is possibly the action stimulating the increase in the number of synaptic boutons in larvae reared at high temperatures. This same behavior has

been observed in the *Drosophila* larva where inducing locomotion activity increased the number of synaptic boutons whereas inducing paralysis decreased them (Sigrist et al. 2003).

Oxygen decrease (normoxic conditions) is certainly the main mechanisms producing the increment of respiratory undulation on high temperature treatments. This was confirmed after inducing the same increase in movement behavior when removing the aeration in the low temperature condition. Although a decrease in the density of boutons was observed in the normoxic treatments as it occurs in high temperature, their effect on the density of boutons resulted different. Induced changes in density of boutons by temperature are mainly affected by changes in the number of boutons, while oxygen induced changes in the density are affected by both, changes in the number of boutons and in the size of the muscles. Increased respiratory undulations are common under reduced oxygen environments too but other changes in metabolic activity and in growth rates have been also reported (Hamburger et al. 1995, Irving et al. 2004) and could be the reason in the change in muscle area in exposed larvae.

These findings of the effects of environmental and biological variables obliges us to conduct any toxicological exposures in specific conditions to reduce confounding effects. Since no effect on age and sex is observed for the density of boutons at 25ºC, this could be the marker studied and the temperature conditions to be used in toxicological trails. Oxygenation should be maintained constant to minimize possible interactions as well. Using the number of boutons and muscle area as markers should be avoided for addressing toxicity with larvae of both sex or with larvae of different sizes, since these markers seem to be influenced by these factors.

Responses to contaminants

The toxicological effect of DBP on the nervous system is barely known. Nevertheless, it is known that exposure to this compound results in reduced locomotory activity in crustaceans (Thurén and Woin 1991, Crooke Rosado et al. 2015). Other similar phthalate ester such as Diethyl phthalate (DEHP) have been observed to alter the neurons properties by inhibiting the calcium channel activity (Ran et al. 2012). The effects of Pb^{2+} in the nervous system is more understood and it has been observed to induce neurotoxicity by oxidative stress (Shilpa et al. 2021), alterations in the presynaptic calcium regulation and changes in synaptic facilitation (He et al. 2009). However, there is little information about what are the effects in the morphology of the NMJ.

This study shows that the presence of DBP and Pb^{2+} in the rearing media induces changes in the NMJ complex. DBP have been shown to act as an endocrine disruptor, capable of interacting with locomotor behaviors in crustaceans (Thurén and Woin 1991) and disrupt development (Memmi and Atlı 2009), fertility (Zhang et al. 2007), and lifespan (Rajamanikyam et al. 2017) on some dipterans. The toxicity effects of DBP in the NMJ of invertebrates are not well understood but this study suggests that some of the effects in the NMJ could be an increase in the number and density of boutons. Possible causes for this could be related to the capacity of DBP and other phthalates of inducing oxidative stress in aquatic animals (Zhang et al. 2021), process that have been linked to contribute with synaptic overgrowth in the *D. melanogaster* larvae (Milton et al. 2011).

Differently to DBP, Pb^{2+} exposure in this study provoked changes in the development of the larvae resulting in smaller larvae with reduced muscle area and high

density of synaptic boutons. Some concentrations of Pb^{2+} are known to provoke developmental delay and affect the size of the larva in the *Chironomus* group (Timmermans et al. 1992, Martinez 2000). Small larvae are expected to have small muscle area but what is interesting here is that the density of boutons was higher than the exposed larvae. The reason of small muscles with increased density of boutons could be attributed to the capacity of Pb^{2+} in affecting Ca^{2+} channel function and Ca^{2+} intracellular and extracellular concentration in the NMJ (He et al. 2009). It has been reported that fewer functional Ca^{2+} channels can produce an increase in bouton number and a decrease in muscle size (Dickman et al. 2008).

It is important to mention that other mechanisms could be involved in how DBP and Pb^{2+} affects the NMJ. However, the most important part here is that the studied NMJ structures are responsive to the toxicity of contaminants and could be used in a future as an established CTM to assess toxicity. Concluding this work and based in our findings we confirm the suitability of *Chironomus* sp. "Florida" to assess sediment toxicity due to its response to contaminated sediments. Although additional work is needed, this first attempt of using a native species and its NMJ for assessing toxicity result of great importance in the Caribbean region due to the lack of ecologically relevant invertebrate models for assessing toxicity.

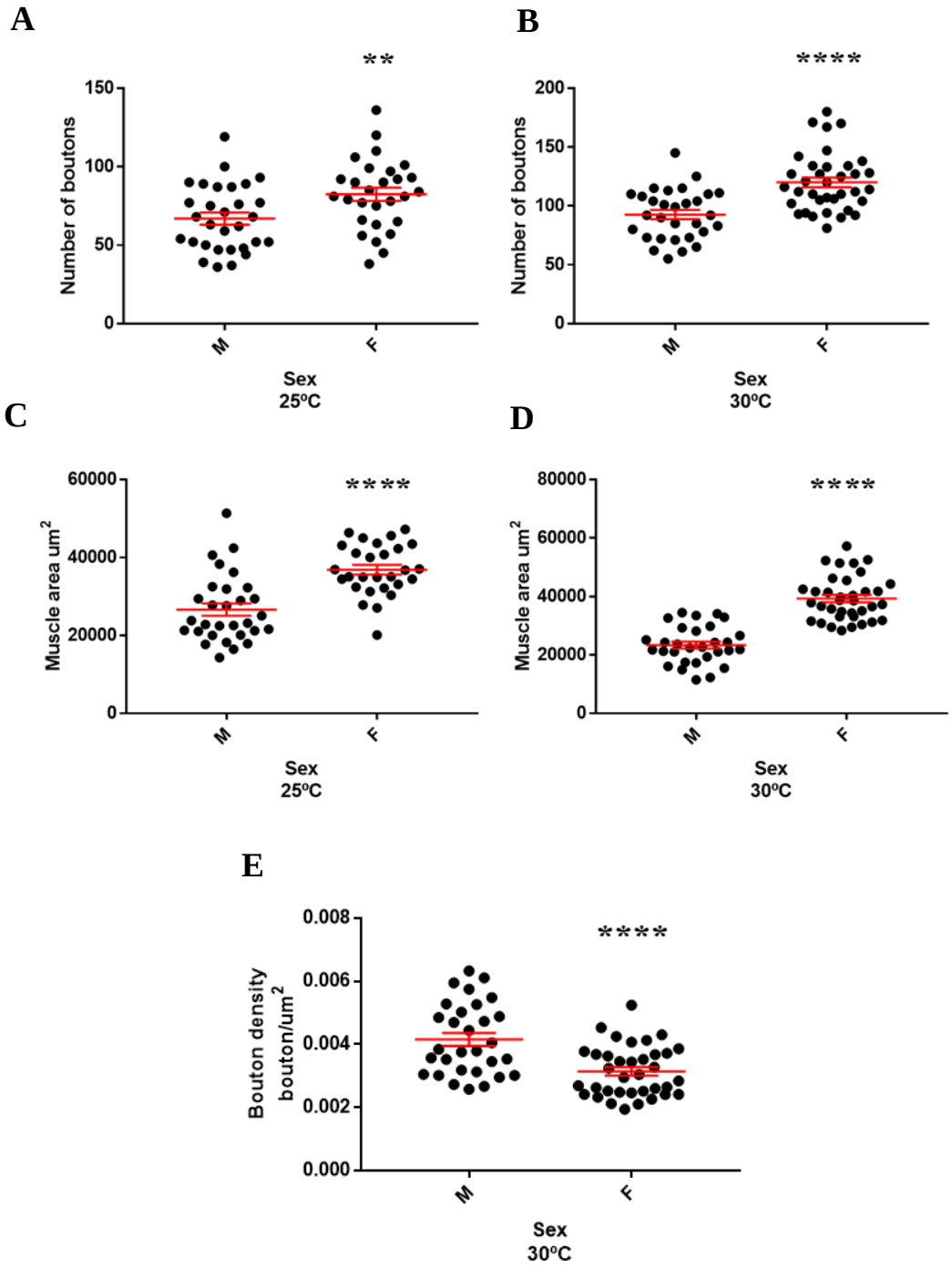

Figure 4.1: Larval sex influence changes in the number of boutons, muscle area and density of boutons. Quantification of the number of boutons (A and B), muscle area (C and D) and density of boutons (E) between males and females reared at 25 (A and C) and 30ºC (B, D and E). **$p < 0.01$; ****$p < 0.0001$. Unpaired T test (A, D and E) and Mann Whitney Test (B and C). Individual data are shown as scatter plots as well as mean ± SEM. Abbreviations M: male, F: Female.

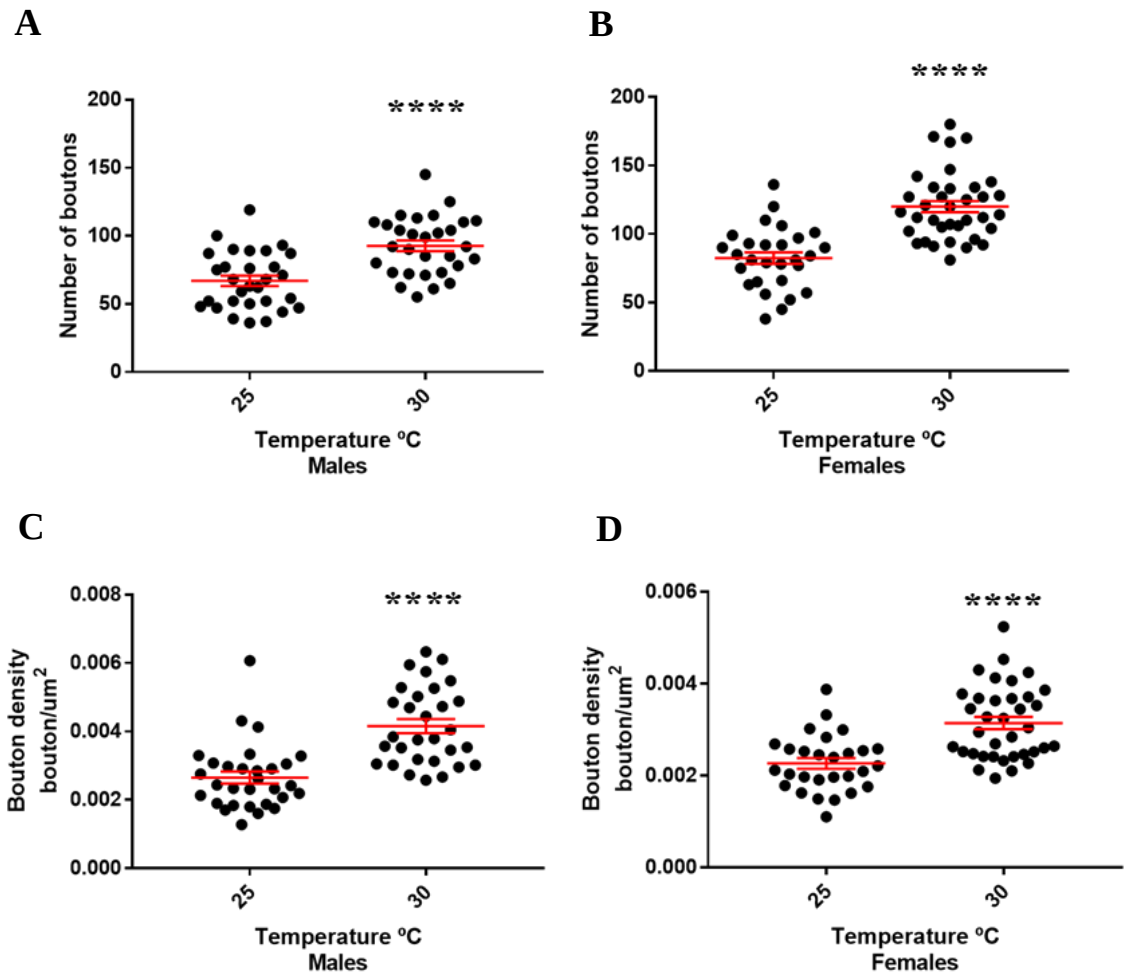

Figure 4.2: Temperature induces changes on the number and density of boutons. Quantification of the number of boutons (A and B) and density of boutons (C and D) between males (A and C) and females (B and D) reared at 25 and 30ºC. ****$p < 0.0001$. Unpaired T test (A and D) and Mann Whitney U test (B and C). Individual data are shown as scatter plots as well as mean ± SEM.

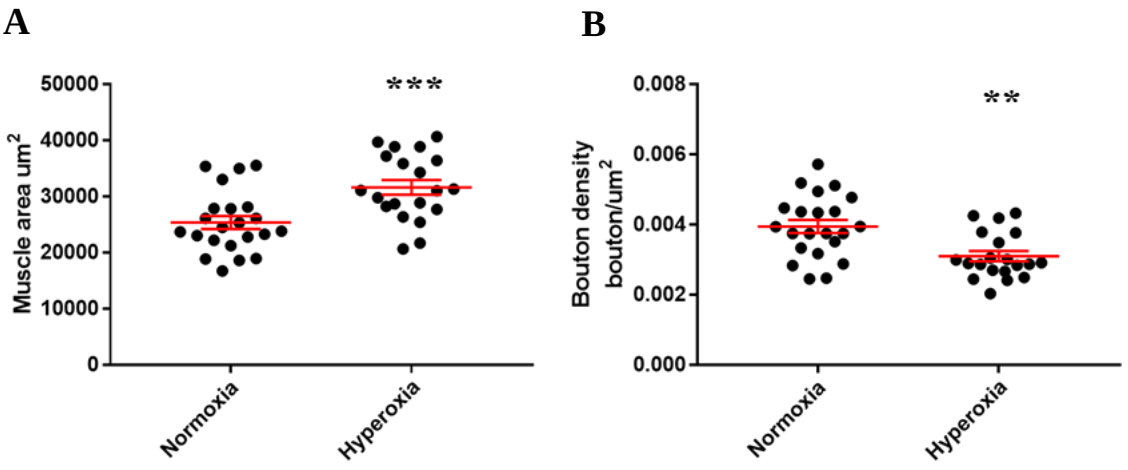

Figure 4.3: Oxygenation induces changes on muscle area and density of boutons. Quantification of the muscle area (A) and density of boutons (B) in larvae exposed to environments differing in oxygenation. **$p < 0.01$; ***$p < 0.001$. Unpaired t-test. Individual data are shown as scatter plots as well as mean ± SEM.

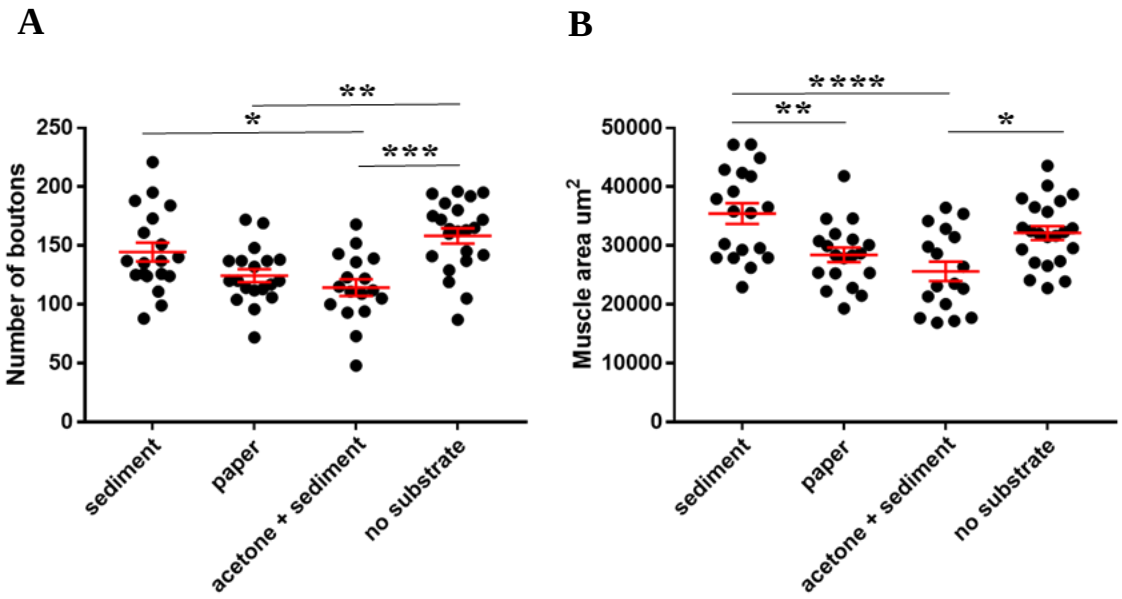

Figure 4.4: Sediment type induces changes on the number of boutons and muscle area. Quantification of the number of boutons (A) and muscle area (B) in larvae exposed to different substrate types. *p<0.05; **p < 0.01; ***p < 0.001; ****p < 0.0001. ANOVA with Tukey's post hoc test. Individual data are shown as scatter plots as well as mean ± SEM.

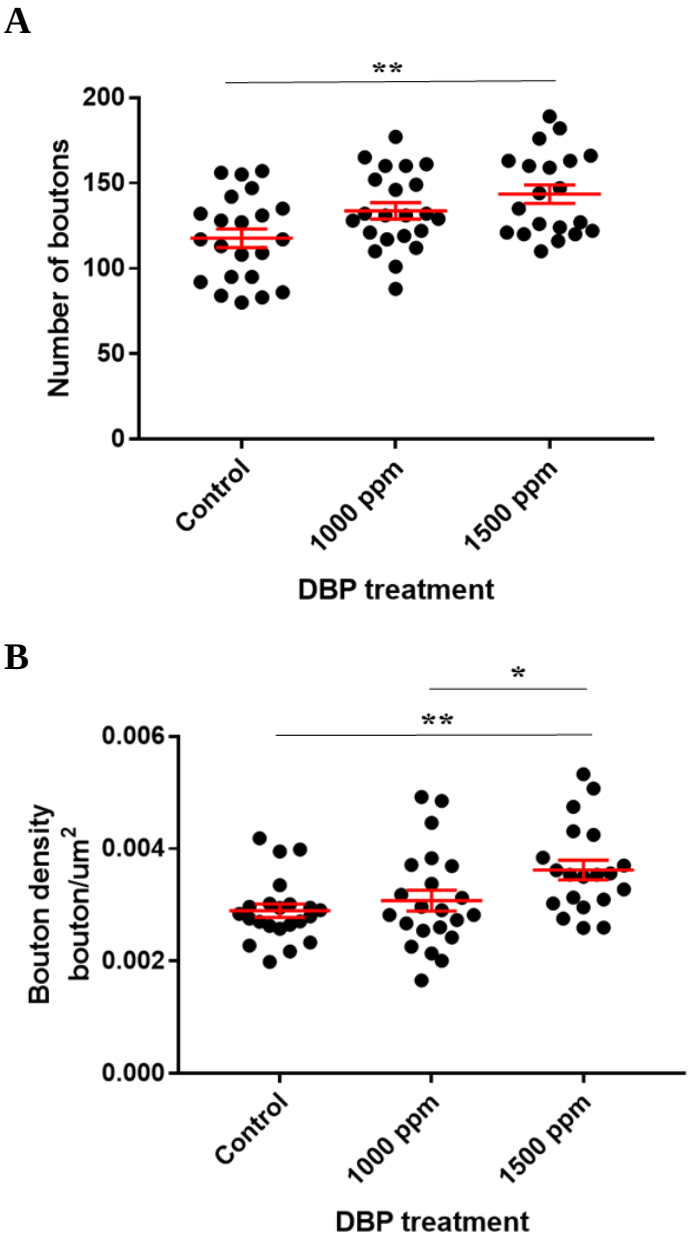

Figure 4.5: High doses of DBP induce changes on the number and density of boutons. Quantification of the number (A) and density (B) of boutons in larvae exposed to three concentrations of DBP spiked sediments. *$p < 0.05$; **$p < 0.01$. ANOVA with Tukey's post hoc test (A) Kruskal-Wallis nonparametric test with Dunn's multiple comparison test (B). Individual data are shown as scatter plots as well as mean ± SEM.

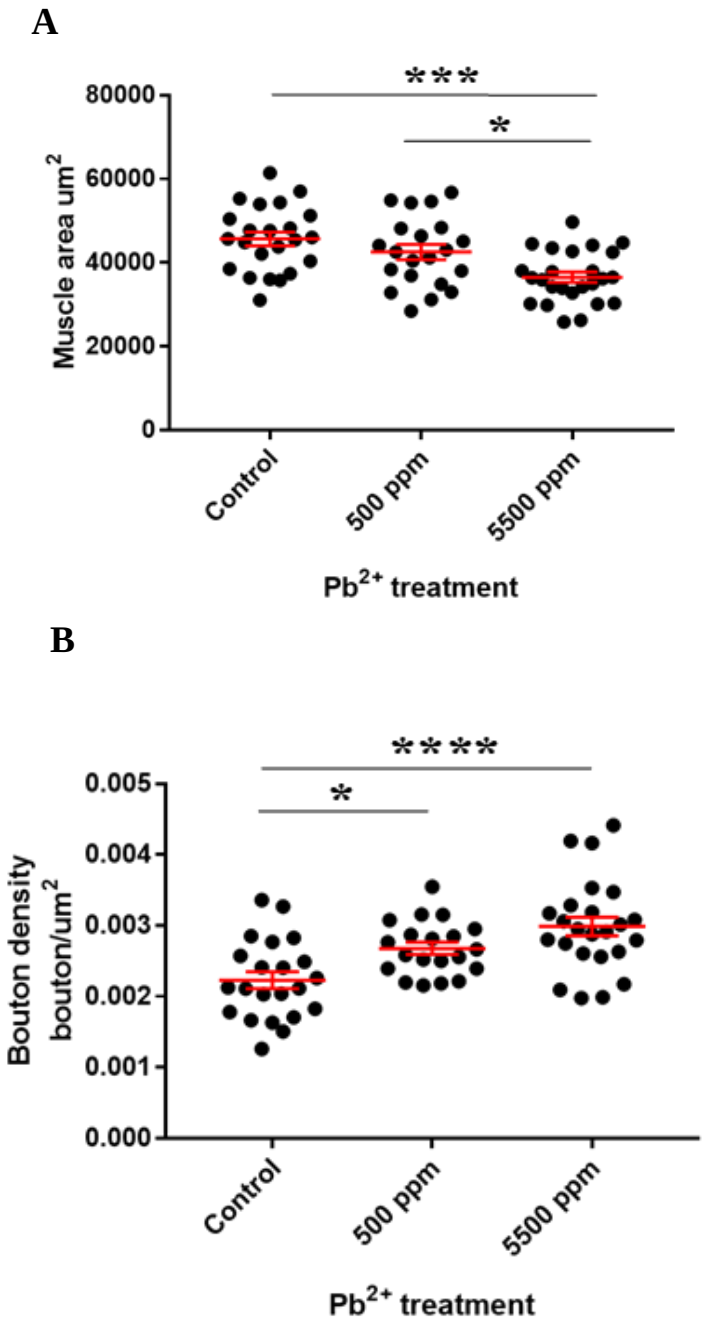

Figure 4.6: High doses of Pb^{2+} induce changes on the muscle area and density of boutons. Quantification of the muscle area (A) and density of boutons (B) in larvae exposed to three concentrations of Pb^{+2} spike sediments. *$p < 0.05$; ***$p < 0.001$. ANOVA with Tukey's post hoc test. Individual data are shown as scatter plots as well as mean ± SEM.

Table 4.1. Sediment particle distribution, organic matter % and dry matter of the substrate used for spiking DBP and Pb^{2+}.

	%
Particle size (mm)	
>2	4.35
>1-2	31.87
>0.5-1	23.37
>0.05-0.5	28.70
<0.05	11.72
Organic content	8.37
Dry matter	66.96

Table 4.2. Analysis on the response of different NMJ parameters (number of boutons, muscle area and density of boutons) to different environmental and biological variables. P values > 0.05 show no significant difference among data. Abbreviations: 20: 20ºC, 30: 30 ºC, ME: 4th Instar early males, ML: 4th Instar late males, FE: 4th Instar early females, FL: 4th Instar late females, M: males, F: females, N: normoxia, H: hyperoxia, S: natural sediment, SP: Shredded paper, SA: natural sediment with acetone, NS: no substrate.

Evaluated Variable	**Relation**	**P value**		
		Number of boutons	**Muscle area**	**Density of boutons**
Age	25ME vs 25ML	>0.05	>0.05	>0.05
	25FE vs 25 FL	>0.05	>0.05	>0.05
	30ME vs 30ML	>0.05	>0.05	>0.05
	30FE vs 30 FL	>0.05	>0.05	>0.05
Sex	25M vs 25F	0.0086	<0.0001	>0.05
	30M vs 30F	<0.0001	<0.0001	<0.0001
Temperature	25M vs 30M	<0.0001	>0.05	<0.0001
	25F vs 30F	<0.0001	>0.05	<0.0001
Oxygenation	N vs H	>0.05	0.001	0.0012
Substrate and Solvent	S. vs SP	>0.05	0.0058	>0.05
	S vs SA	0.0165	<0.0001	>0.05
	S vs NS	>0.05	>0.05	>0.05
	SP vs SA	>0.05	>0.05	>0.05
	SP vs NS	0.0028	>0.05	>0.05
	NS vs SA	0.001	0.013	>0.05

Table 4.3. Average water parameters recorded during the toxicity assay with DBP and Pb^{2+}. Mean and standard deviations were calculated by analyzing data obtained through time and replicas.

	pH Mean ± σ	Conductivity uS/cm Mean ± σ	NH3 (mg/L) Mean ± σ	Alkalinity (mg/L CaCO3) Mean ± σ	Hardness (mmol/L HCO3-) Mean ± σ
$DBP_{Control}$	7.2 ± 0.10	217 ±6.87	0.4 ± 0.13	92 ± 2.89	97 ± 3.84
DBP_{1000}	7.2 ± 0.07	337 ± 1.88	0.2 ± 0.07	90 ±0	103 ± 3.84
DBP_{1500}	7.3 ± 0.04	230 ± 13.01	0.2 ± 0.06	88 ±2.89	103 ± 1.76
$Pb^{2+}_{Control}$	7.5 ± 0.10	289 ± 3.88	1.3 ± 0	115 ± 0	130 ± 4.66
Pb^{2+}_{500}	7.5 ± 0.06	329 ± 4.30	1.1 ± 0	101 ± 2.89	128 ± 5.36
Pb^{2+}_{5500}	7.1 ±0.07	873 ± 32.89	0.6 ± 0.03	80 ± 0	89 ± 7.94

Table 4.4: Nominal concentrations of DBP and Pb^{2+} used during the toxicity assay and the respective average and deviation standard of the number of boutons, muscle area and density of boutons obtained from larvae exposed to these concentrations.

Treatment	Nominal concentration (ppm)	Number of boutons Mean ± σ	Muscle area (um^2) Mean ± σ	Density of boutons (Bouton number/um^2) Mean ± σ
$DBP_{Control}$	0	117.7 ± 25.24	41234 ± 8526	$2.897 \times 10^{-3} \pm 5.614 \times 10^{-4}$
DBP_{1000}	1000	133.8 ± 22.64	46138 ± 11792	$3.077 \times 10^{-3} \pm 8.740 \times 10^{-4}$
DBP_{1500}	1500	143.5 ± 24.48	40566 ± 7038	$3.623 \times 10^{-3} \pm 7.787 \times 10^{-4}$
$Pb^{2+}_{Control}$	0	99.59 ± 20.72	45673 ± 7803	$2.228 \times 10^{-3} \pm 5.578 \times 10^{-4}$
Pb^{2+}_{500}	500	112.5 ± 19.69	42537 ± 8302	$2.678 \times 10^{-3} \pm 3.797 \times 10^{-4}$
Pb^{2+}_{5500}	5500	106.5 ± 16.75	36528 ± 6170	$2.988 \times 10^{-3} \pm 6.484 \times 10^{-4}$

Table 4.5: Analysis on the response of different NMJ parameters (number of boutons, muscle area and density of boutons) to different nominal concentrations of DBP and Pb^{2+}. P values > 0.05 show no significant difference among data. The plus and minus signs (+ and -) show significant increases or decreases in the values of the NMJ parameters when compared between treatments.

Evaluated Variable	Relation	P value		
		Number of boutons	Muscle area	Density of boutons
DBP	$DBP_{Control}$ vs. DBP_{1000}	>0.05	>0.05	>0.05
	$DBP_{Control}$ vs. DBP_{1500}	0.0028 (+)	>0.05	0.0069 (+)
	DBP_{1000} vs DBP_{1500}	>0.05	>0.05	0.0472 (+)
Pb^{2+}	$Pb^{2+}_{Control}$ vs. Pb^{2+}_{500}	>0.05	>0.05	0.0267
	$Pb^{2+}_{Control}$ vs. Pb^{2+}_{5500}	>0.05	0.0002 (-)	<0.0001 (+)
	Pb^{2+}_{500} vs Pb^{2+}_{5500}	>0.05	0.0215 (-)	>0.05

CHAPTER 5

General Discussion

Different molecular, biochemical and morphological markers are used to determine toxicity in aquatic environments when using chironomids as models (Martinez et al. 2004, Lee et al. 2006, Dias et al. 2008, Park and Kwak 2008). The use of cellular and tissue markers is rarely seen when evaluating toxicity, but their implementation could help to identify toxicity faster than when using morphological markers and could address toxicity in a more cost-effective way than when using molecular and biochemical markers. Cellular structures such as the neuromuscular junction (NMJ) are of interest for use as cellular and tissue markers given its relation to movement, response to external factors and variety of quantifiable features.

In this thesis, we have addressed the suitability of the *Chironomus* NMJ as cellular and tissue marker (CTM) for assessing benthic sediment toxicity. We have used the neotropical larvae of *Chironomus* sp. "Florida", a prospective chironomid model for assessing toxicity in Puerto Rico. Although this chironomid has not been validated as a laboratory model, its use in aquatic toxicological assays in Puerto Rico represents a better option than using any other established exotic aquatic model since local species are better adapted to local environmental conditions (Freitas and Rocha, 2011). The use of exotic models in tropical regions is also dangerous since they could become invasive species if released accidentally to the environment (Freitas and Rocha, 2011). As shown in Chapter 2, this chironomid could be used to assess chronic effects of contaminants in a short period of time (approximately a week) based on the short life cycle of the insect. These short

chronic assays would be a benefit for the toxicology field since they compare drastically for the long-time effort required when assessing toxicity with temperate zone chironomid models such as *C. riparius* and *C. tentans*.

To achieve the main goal of this project it was necessary to make a description of the neuromuscular anatomy of *Chironomus* sp. "Florida" in order to identify a model NMJ and use it as a quantifiable CTM. The present work addressed this on Chapter 3, and the muscle area, the number of synaptic boutons and the density of synaptic boutons in the NMJ were selected as markers given their easy study and quantification. Having this description not only opens the possibility of identifying new cell markers for toxicity purposes but could also help in the development of new protocols to study nervous function and how this is affected by pollutants. Other applications may arise in the neuroscience and comparative biology field given the easy study of the system and the similarities that it has with the neuromuscular system of other insects.

The results presented in Chapter 4, indicates that *Chironomus* sp. "Florida" is a sensitive chironomid at the nervous cellular level. Quantifying the muscle area, number of boutons and the density of boutons in the *Chironomus* NMJ resulted in the detection of high chemical doses of dibutyl phthalate and lead in spiked benthic sediments. These chemicals acted as neurotoxicants, affecting mainly the density of boutons in the NMJ. Changes observed in the density of boutons were possibly caused by induced changes at molecular level than by behavioral changes itself. Nevertheless, more studies are needed in order to confirm this premise and discard the idea that induced changes in behavior are affecting the NMJ features. Here it was established that quantifying the density of boutons

specifically, provide better insights to detect toxicity since this marker seems to be less influenced by biological factors such as larval sex and size. However, in future toxicological studies using this model, environmental parameters should be maintained stable to reduce their impact on the NMJ.

Although our results provide evidence for using the NMJ as a tissue for evaluating toxicity our findings are difficult to compare with other studies given the lack of research using the same markers and chemicals that were evaluated in this work. Other limitation of this work was that the exact concentration of the contaminant in the sediment or in the water media was not measured. This partially limits our study since we were not able to define with certainty those concentrations that were inducing the changes in the studied marker. For this reason, we encourage the preparation of new validations determining the chemical concentration in the media when assessing toxicity. The future validation of the NMJ features as maker for assessing contaminants dissolved in water is also encouraged, since the water media is also a known source of contaminants in the environment.

Together, the addressed aims in this study have helped in the establishment of some NMJ component as markers for assessing toxicity in benthic sediments. Also, a new model organism has been recommended for pursuing toxicological tests in Puerto Rico. Having a new model and a new cellular marker provide us with an inexpensive tool for assessing freshwater environments and contaminants in the island. Similarly, the inputs received through the description of the nervous system of *Chironomus sp. "Florida"* will encourage for sure the development of additional studies in the field of toxicology, neuroscience, and comparative biology.

REFERENCES

Abashy, M. M. 2005. Culture of chironomid larvae (Insecta- Diptera Chironomidae) under different feeding systems. Egyptian Journal of Aquatic Research 31:403–418.

Al-Shami, S., C. S. M. Rawi, S. A. M. Nor, A. H. Ahmad, and A. Ali. 2010. Morphological deformities in Chironomus spp. (Diptera: Chironomidae) larvae as a tool for impact assessment of anthropogenic and environmental stresses on three rivers in the Juru River System, Penang, Malaysia. Environmental Entomology 39:210–222.

Arambourou, H., J. N. Beisel, P. Branchu, and V. Debat. 2012. Patterns of Fluctuating Asymmetry and Shape Variation in Chironomus riparius (Diptera, Chironomidae) Exposed to Nonylphenol or Lead. PLoS ONE 7.

Arambourou, H., E. Gismondi, P. Branchu, and J. N. Beisel. 2013. Biochemical and morphological responses in Chironomus riparius (Diptera, Chironomidae) larvae exposed to lead-spiked sediment. Environmental Toxicology and Chemistry 32:2558–2564.

Armitage, P. D., P. S. Cranston, and L. C. v. Pinder. 1995. The Chironomidae: Biology and ecology of non-biting midges. Page The Chironomidae: biology and ecology of non-biting midges. First edit. Springer Science & Business Media, United Kingdom.

Atwood, H. L., and R. L. Cooper. 1996. Synaptic diversity and differentiation: crustacean neuromuscular junctions. Invertebrate Neuroscience 1:291–307.

Azevedo-Pereira, H. M. V. S., and A. M. V. M. Soares. 2010. Effects of mercury on growth, emergence, and behavior of Chironomus riparius Meigen (Diptera: Chironomidae). Archives of environmental contamination and toxicology 59:216–224.

Baptista, D. F., A. L. Henriques-Oliveira, R. B. S. Oliveira, R. Mugnai, J. L. Nessimian, and D. F. Buss. 2013. Development of a benthic multimetric index for the Serra da Bocaina bioregion in Southeast Brazil. Brazilian Journal of Biology 73:573–583.

Baranov, V., J. Lewandowski, and S. Krause. 2016. Bioturbation enhances the aerobic respiration of lake sediments in warming lakes. Biology letters 12:20160448.

Batac-Catalan, Z., and D. S. White. 1982. Creating and maintaining cultures of Chironomus tentans (Diptera: Chironomidae). Entomological news 93:54–58.

Bate, M. 1993. The mesoderm and its derivative. Pages 1013– 1090 *in* M. (Bate and A. Martinez Arias, editors. The development of Drosophila melanogaster. Cold Spring Harbor Laboratory Press.

Beckett, K., and M. K. Baylies. 2006. The Development of The Drosophila Larval Body Wall Muscles. International Review of Neurobiology 75:55–70.

Bello González, O., M. Spies, and B. Téllez. 2013. Estado del conocimiento de la familia Chironomidae (Insecta:Diptera) en Cuba. Dugesiana 20:233–242.

Benoit, J. B., G. Lopez-Martinez, M. A. Elnitsky, R. E. Lee, and D. L. Denlinger. 2007. Moist habitats are essential for adults of the antarctic midge, Belgica antarctica (Diptera: Chironomidae), to avoid dehydration. European Journal of Entomology 104:9–14.

Berg, M. B. 1995. Larval food and feeding behaviour. Pages 136–168 *in* P. D. Armitage, editor. The Chironomidae: biology and ecology of non-biting midges. Springer.

Bhaduri, S., P. Sarkar, C. Ghosh, and T. Midya. 2012. Laboratory Rearing of Chironomus striatipennis Kieffer (Diptera: Chironomidae). Proceedings of the Zoological Society 65:121–125.

Biever, K. D. 1965. A rearing technique for the colonization of chironomid midges. Annals of the Entomological Society of America 58:135–136.

Biever, K. D. 1971. Effect of diet and competition in laboratory rearing of chironomid midges. Annals of the Entomological Society of America 64:1166–1169.

Bird G.A. 1997 Deformities in cultured chironomus tentanslarvae and the influence of substrate on growth, survival and mentum wear. Environ Monit Assess 45:273–283.

Brown, D., R. S. Thompson, K. M. Stewart, C. P. Croudace, and E. Gillings. 1996. The effect of phthalate ester plasticisers on the emergence of the midge (Chironomus riparius) from treated sediments. Chemosphere 32:2177–2187.

Budnik, V., Y. Zhong, and C.-F. Wu. 1990. Morphological plasticity of motor axons in Drosophila mutants with altered excitability. Journal of Neuroscience 10:3754–3768.

Buso, C., S. Rodgher, R. Galante Negri, E. L. Gaeta Espíndola, and M. A. Daam. 2018. Chironomus sancticaroli (Diptera, Chironomidae) as a sensitive tropical test species in laboratory bioassays evaluating metals (copper and cadmium) and field testing. Archives of Environmental Contamination and Toxicology 76:42–50.

Buttermore, E. 2011. Contaminant and Trophic Dynamics of Tropical Stream Ecosystems. North Carolina State University.

Call, D. J., D. A. Cox, D. L. Geiger, K. I. Genisot, T. P. Markee, L. T. Brooke, C. N. Polkinghorne, F. A. VandeVenter, J. W. Gorsuch, K. A. Robillard, T. F. Parkerton, M. C. Reiley, G. T. Ankley, and D. R. Mount. 2001a. An assessment of the toxicity of phthalate esters to freshwater benthos. 2. Sediment exposures. Environmental Toxicology and Chemistry 20:1805–1815.

Call, D. J., T. P. Markee, D. L. Geiger, L. T. Brooke, F. A. VandeVenter, D. A. Cox, K. I. Genisot, K. A. Robillard, J. W. Gorsuch, T. F. Parkerton, M. C. Reiley, G. T. Ankley, and D. R. Mount. 2001b. An assessment of the toxicity of phthalate esters

to freshwater benthos. 1. Aqueous exposures. Environmental Toxicology and Chemistry 20:1798–1804.

Campbell, M., and B. Ganetzky. 2013. Identification of Mob2, a novel regulator of larval neuromuscular junction morphology, in natural populations of Drosophila melanogaster. Genetics 195:915–926.

Canteiro, R. C. S. A., and E. F. Albertoni. 2011. Growth of immature chironomus calligraphus (diptera, chironomidae) in laboratory conditions. Anais da Academia Brasileira de Ciencias 83:1279–1286.

Chockalingam, V., D. Radhika, and D. Kumar. 2006. Lifecycle and larval rearing of Chironomous ramosus using different organic nutrients. Environment and Ecology 24:373–378.

Collins, C. A., and A. DiAntonio. 2007. Synaptic development: insights from Drosophila. Current Opinion in Neurobiology 17:35–42.

Colón-Cruz, L., L. Kristofco, J. Crooke-Rosado, A. Acevedo, A. Torrado, B. W. Brooks, M. A. Sosa, and M. Behra. 2018. Alterations of larval photo-dependent swimming responses (PDR): New endpoints for rapid and diagnostic screening of aquatic contamination. Ecotoxicology and Environmental Safety 147:670–680.

Corbi, J. J., and S. Trivinho-Strixino. 2006. Life cycle of two Goeldichironomus species (Diptera, Chironomidae). Revista Brasileira de Entomologia 50:72–75.

Cranston, P. S. 2004. Insecta: Diptera, Chironomidae. Pages 710–734 *in* C. M. Yule and H. sen Yong, editors. The freshwater invertebrates of the Malaysia region.

Crooke Rosado, J., N. Rivera Chéverez, and M. Sosa Llorens. 2015. Use of Freshwater Prawn Larval Locomotor Activity and Electrophysiological Recording at the Adult Neuromuscular Junction to Assess the Effects of Urban River Contaminants on Behavior and Nervous System Function. The FASEB Journal 29:542–543.

Dejoux, C. 1971. Recherches sur le cycle de developpement de Chironoimus pulcher (Diptera: Chironomidae). The Canadian Enthomologist 103:465–470.

Dias, V., C. Vasseur, and J. M. Bonzom. 2008. Exposure of Chironomus riparius larvae to uranium: Effects on survival, development time, growth, and mouthpart deformities. Chemosphere 71:574–581.

Dickman, D. K., P. T. Kurshan, and T. L. Schwarz. 2008. Mutations in a drosophila 2 voltage-gated calcium channel subunit reveal a crucial synaptic function. Journal of Neuroscience 28:31–38.

Dyar, H. G. 1890. The Number of Molts of Lepidopterous Larvae. Psyche 5:420–422.

Epler, J. H. 2001. Identification manual for the larval Chironomidae (Diptera) of North and South Carolina. John H. Epler, Crawford, South Carolina.

Férard, J. F., and C. Blaise. 2013. Encyclopedia of Aquatic Ecotoxicology. Springer Netherlands.

Ferrington, L. C. Jr., K. M. Buzby, and E. C. Masteller. 1993. Composition and Temporal Abundance of Chironomidae Emergence from a Tropical Rainforest Stream at El Verde , Puerto Rico. Journal of the Kansas Entomological Society 66:167–180.

Fittkau, E. J. 1968. Chironomus strenzkei n. sp. (Chironomidae, Dipt.), ein neues Laboratoriumstier. Zeitschrift für Morphologie der Tiere 63:239–250.

Fonseca, A. L., and O. Rocha. 2004. Laboratory cultures of the native species Chironomus xanthus Rempel, 1939 (Diptera-Chironomidae). Acta Limnologica Brasiliensia 16:153–161.

Forbes, V. E., A. Palmqvist, and L. Bach. 2006. The use and misuse of biomarkers in ecotoxicology. Environmental Toxicology and Chemistry 25:272–280.

Freitas, E. C., and O. Rocha. 2011. Acute toxicity tests with the tropical cladoceran Pseudosida ramosa: The importance of using native species as test organisms. Archives of Environmental Contamination and Toxicology 60:241–249.

Frouz, J., A. Ali, and R. J. Lobinske. 2002. Suitability of morphological parameters for instar determination of pestiferous midges Chironomus crassicaudatus and Glyptotendipes paripes (Diptera: Chironomidae) under laboratory conditions. Journal of the American Mosquito Control Association 18:222–227.

Gautreau, E., L. Volatier, G. Nogaro, E. Gouze, and F. Mermillod-Blondin. 2020. The influence of bioturbation and water column oxygenation on nutrient recycling in reservoir sediments. Hydrobiologia 847:1027–1040.

Gerhardt, A., and L. J. de Bisthoven. 1995. Behavioural , developmental and morphological responses of Chironomus gr . thummi larvae (Diptera , Nematocera) to aquatic pollution. Journal of Aquatic Ecosystem Health 4:205–214.

Gibbs, M., and H. van Dyck. 2010. Butterfly flight activity affects reproductive performance and longevity relative to landscape structure. Oecologia 163:341–350.

Goedkoop, W., N. Spann. 2010. Sublethal and sex-specific cypermethrin effects in toxicity tests with the midge Chironomus riparius Meigen. :1201–1208.

Green, A. J., and A. Planchart. 2018. The neurological toxicity of heavy metals: A fish perspective. Comparative Biochemistry and Physiology Part C: Toxicology & Pharmacology 208:12–19.

Grosell, M., R. M. Gerdes, and K. v Brix. 2006. Chronic toxicity of lead to three freshwater invertebrates—Brachionus calyciflorus, Chironomus tentans, and Lymnaea stagnalis. Environmental Toxicology and Chemistry: An International Journal 25:97–104.

De Haas, E. M., R. Van Haaren, A. A. Koelmans, M. H. S. Kraak, and W. Admiraal. 2005. Analyzing the causes for the persistence of chironomids in floodplain lake sediments. Archiv fur Hydrobiologie 162:211–228.

Hamburger, K., P. C. Dall, and C. Lindegaard. 1995. Effects of oxygen deficiency on survival and glycogen content of Chironomus anthracinus (Diptera, Chironomidae) under laboratory and field conditions. Hydrobiologia 297:187–200.

He, T., H. V. B. Hirsch, D. M. Ruden, and G. A. Lnenicka. 2009. Chronic lead exposure alters presynaptic calcium regulation and synaptic facilitation in Drosophila larvae. Neurotoxicology. 30:777–784.

He, Y., W. Lin, C. Shi, R. Li, C. Mu, C. Wang, and Y. Ye. 2022. Accumulation, detoxification, and toxicity of dibutyl phthalate in the swimming crab. Chemosphere 289:133183.

Hein, J., and M. N. Mahadeva. 1992. Rearing & maintaining midge cultures (Chironomus tentans) for laboratory studies. The American Biology Teach 54:236–240.

Hirsch, H. V. B., G. Lnenicka, D. Possidente, B. Possidente, M. D. Garfinkel, L. Wang, X. Lu, and D. M. Ruden. 2012. Drosophila melanogaster as a model for lead neurotoxicology and toxicogenomics research. Frontiers in Genetics 3:1–7.

Hoyle, G. 1954. The anatomy and innervation of locust skeletal muscle.

Inal, M. A., K. Banzai, and D. Kamiyama. 2020. Retrograde tracing of Drosophila embryonic motor neurons using lipophilic fluorescent dyes. JoVE (Journal of Visualized Experiments):e60716.

Ingersoll, C. G., G. T. Ankley, G. A. Burton, F. J. Dwyer, R. A. Hoke, T. J. Norberg-King, and P. V. Winger. 2000. Methods for Measuring the Toxicity and Bioaccumulation of Sediment-associated Contaminants with Freshwater Invertebrates. Second edi. US Environmental Protection Agency, Duluth, Minnesota.

Irving, E. C., K. Liber, and J. M. Culp. 2004. Lethal and sublethal effects of low dissolved oxygen condition on two aquatic invertebrates, Chironomus tentans and Hyalella azteca. Environmental Toxicology and Chemistry: An International Journal 23:1561–1566.

Johansson, O., A. Olsson, and L. Wieslander. 1986. The distribution of putative neurotransmitters in the nervous system of the dipteran Chironomus tentans insect larva: An immunohistochemical study using antisera to 5-hydroxytryptamine, tyrosine hydroxylase, methionine-enkephalin, proctolin and bombesin. Neurochemistry International 8:311–326.

Kim, J.-H., and J.-C. Kang. 2017. Toxic effects on bioaccumulation and hematological parameters of juvenile rockfish Sebastes schlegelii exposed to dietary lead (Pb) and ascorbic acid. Chemosphere 176:131–140.

Kuhlmann, M. L., C. Y. Hayashida, and R. P. A. Araújo. 2000. Using Chironomus (Chironomidae: Diptera) deformities in environmental assessment. Acta Limnologica Brasiliensia 12:55–56.

Landgraf, M., T. Bossing, G. M. Technau, and M. Bate. 1997. The origin, location, and projections of the embryonic abdominal motorneurons of Drosophila. Journal of Neuroscience 17:9642–9655.

Laurindo da Silva, F., S. Wiedenbrug, and B. D. Farrell. 2015. A preliminary survey of the non-biting midges (Diptera: Chironomidae) of the Dominican Republic. Journal of Chironomidae Research:12–19.

Lee, J.-W., H. Choi, U.-K. Hwang, J.-C. Kang, Y. J. Kang, K. il Kim, and J.-H. Kim. 2019. Toxic effects of lead exposure on bioaccumulation, oxidative stress, neurotoxicity, and immune responses in fish: A review. Environmental toxicology and pharmacology 68:101–108.

Lee, S.-M., S.-B. Lee, C.-H. Park, and J. Choi. 2006. Expression of heat shock protein and hemoglobin genes in Chironomus tentans (Diptera, chironomidae) larvae exposed to various environmental pollutants: a potential biomarker of freshwater monitoring. Chemosphere 65:1074–1081.

Lencioni, V., F. Bellamoli, P. Bernabò, F. Miari, and A. Scotti. 2018. Response of Diamesa spp. (Diptera: Chironomidae) from alpine streams to newly emergent contaminants and pesticides. Journal of Limnology 77:131–140.

de León, J., M. D. C. Cotto, C. J. Olivo, and F. M. Márquez. 2020. Effects of chronic environmental exposure to waterborne lead and copper on the dopaminergic and serotonergic systems of zebrafish. Toxicology and Environmental Health Sciences 12:265–272.

Lerner, A., N. Meltser, N. Sapir, C. Erlick, N. Shashar, and M. Broza. 2008. Reflected polarization guides chironomid females to oviposition sites. Journal of Experimental Biology 211:3536–3543.

Letinsky, M. S., and K. Morrison-Graham. 1980. Structure of developing frog neuromuscular junctions. Journal of Neurocytology 9:321–342.

Lnenicka, G. A., K. Theriault, and R. Monroe. 2006. Sexual Differentiation of Identified Motor Terminals in Drosophila Larvae. Journal of Neurobiology 14:1564–1583.

Lu, Y., M. Lin, and R. J. Aitken. 2017. Exposure of spermatozoa to dibutyl phthalate induces abnormal embryonic development in a marine invertebrate Galeolaria caespitosa (Polychaeta: Serpulidae). Aquatic Toxicology 191:189–200.

Lyons, P. R., and C. R. Slater. 1991. Structure and function of the neuromuscular junction in young adultmdx mice. Journal of neurocytology 20:969–981.

Maciorowski, H. D., and R. M. V Clarke. 1980. Advantages and Disadvantages of Using Invertebrates in Toxicity Testing. Pages 36–47 *in* A. L. Buikema and J. Cairns, editors. Aquatic Invertebrate Bioassays. ASTM International, West Conshohocken, PA.

Maier, K. J., P. Kosalwat, and A. W. Knight. 1990. Culture of Chironomus decorus (Diptera: Chironomidae) and the effect of temperature on its life history. Environmental Entomology 19:1681–1688.

Martinez, E. A. 2000. Morphological abnormalities and developmental responses in Chironomus tentans exposed to zinc and lead. Washington State University.

Martinez, E. A., B. C. Moore, J. Schaumloffel, and N. Dasgupta. 2001. Induction of morphological deformities in Chironomus tentans exposed to zinc- and lead-spiked sediments. Environmental Toxicology and Chemistry 20:2475–2481.

Martinez, E. A., B. C. Moore, J. Schaumloffel, and N. Dasgupta. 2004. Effects of exposure to a combination of zinc- and lead-spiked sediments on mouthpart development and growth in Chironomus tentans. Environmental Toxicology and Chemistry 23:662–667.

Martínez-Guitarte, J.L., R. Planelló, G. Morcillo. 2007. Characterization and expression during development and under environmental stress of the genes encoding ribosomal proteins L11 and L13 in Chironomus riparius. Comp Biochem Physiol - B Biochem Mol Biol 147:590–596.

Memmi, B. K., and E. Atlı. 2009. The effects of dibutyl phthalate on the development of Drosophila melanogaster. Drosophila information center 92:114.

Menon, K. P., R. A. Carrillo, and K. Zinn. 2013. Development and plasticity of the Drosophila larval neuromuscular junction. Wiley Interdisciplinary Reviews: Developmental Biology 2:647–670.

Meregalli, G., A. C. Vermeulen, and F. Ollevier. 2000. The use of chironomid deformation in an in situ test for sediment toxicity. Ecotoxicology and Environmental Safety 47:231–238.

Miall, L. C., and A. R. Hammond. 1900. The structure and life-history of the harlequin fly (Chironomus). Clarendon Press.

Milton, V. J., H. E. Jarrett, K. Gowers, S. Chalak, L. Briggs, I. M. Robinson, and S. T. Sweeney. 2011. Oxidative stress induces overgrowth of the Drosophila neuromuscular junction. Proceedings of the National Academy of Sciences 108:17521–17526.

Morley, E. J., H. V. B. Hirsch, K. Hollocher, and G. A. Lnenicka. 2003. Effects of chronic lead exposure on the neuromuscular junction in Drosophila larvae. NeuroToxicology 24:35–41.

Murphy, D. J., M. H. Hall, C. A. S. Hall, G. M. Heisler, S. v. Stehman, and C. Anselmi-Molina. 2011. The relationship between land cover and the urban heat island in northeastern Puerto Rico. International Journal of Climatology 31:1222–1239.

Nath, B. B., L. Thorat, A. Babrekar, K. Datkhile, A. Ghadge, R. Gaikwad, and D. C. Meshram. 2009. Development of a new design of an insectary model for rearing and environmental assessment studies on chironomid midges. Chironomus Newsletter on Chironomidae Research 22:11–13.

Naylor, C., and C. Rodrigues. 1995. Development of a test method for Chironomus riparius using a formulated sediment. Chemosphere 31:3291–3303.

New, B. M., J. P. Scholl, J. C. McCarty, and J. P. Bennett. 1974. A recirculation system for experimental aquaria. Aquaculture 3:95–103.

Newman, M. C. 2014. Fundamentals of ecotoxicology: the science of pollution. CRC press.

Nolte, U. 1993. Egg masses of Chironomidae (Diptera). A review including new observations and a preliminary key. Entomologica Scandinavia Supplement 43:1–75.

Ortiz Lugo, J. L., and M. A. C. Sosa Lloréns. 2015. Impacts of urbanization and river water contaminants on abundance, locomotion and aggression of a local freshwater crustacean. University of Puerto Rico.

Ortiz-Colón, A. I., L. E. Piñero-Santiago, N. M. Rivera, and M. A. Sosa. 2016. Assessment of Concentrations of Heavy Metals and Phthalates in Two Urban Rivers of the Northeast of Puerto Rico. Journal of environmental & analytical toxicology 6:1–10.

Osmulski, P. A., and W. Leyko. 1986. Structure, function and physiological role of Chironomus haemoglobin. Comparative Biochemistry and Physiology -- Part B: Biochemistry and 85:701–722.

Ospina-pérez, E. M., O. I. Campeon-Morales, V. S. Richardi, and F. A. Rivera-páez. 2019. Histological description of immature Chironomus columbiensis (Diptera : Chironomidae): A potential contribution to environmental monitoring:1–13.

Park, K., and I.-S. Kwak. 2008. Characterization of heat shock protein 40 and 90 in Chironomus riparius larvae: effects of di (2-ethylhexyl) phthalate exposure on gene expressions and mouthpart deformities. Chemosphere 74:89–95.

Peck, M. R., D. A. Klessa, and D. J. Baird. 2002. A tropical sediment toxicity test using the dipteran Chironomus crassiforceps to test metal bioavailability with sediment pH change in tropical acid-sulfate sediments. Environmental Toxicology and Chemistry 21:720–728.

Péry, A. R. R., and J. Garric. 2006. Modelling effects of temperature and feeding level on the life cycle of the midge Chironomus riparius: An energy-based modelling approach. Hydrobiologia 553:59–66.

Péry, A. R. R., R. Mons, P. Flammarion, L. Lagadic, and J. Garric. 2002. A modeling approach to link food availability, growth, emergence, and reproduction for the midge Chironomus riparius. Environmental Toxicology and Chemistry 21:2507–2513.

Pinder, L. C. V. 1995. The habitats of chironomid larvae. Pages 107–135 *in* P. D. Armitage, editor. The Chironomidae: biology and ecology of non-biting midges. Springer.

Rajamanikyam, M., V. Vadlapudi, S. P. Parvathaneni, D. Koude, P. Sripadi, S. Misra, R. Amanchy, and S. M. Upadhyayula. 2017. Isolation and characterization of phthalates from Brevibacterium mcbrellneri that cause cytotoxicity and cell cycle arrest. EXCLI journal 16:375.

Ran, D., S. Cai, H. Wu, and H. Gu. 2012. Di (2-ethylhexyl) phthalate modulates cholinergic mini-presynaptic transmission of projection neurons in Drosophila antennal lobe. Food and chemical toxicology 50:3291–3297.

Randall, W. C. 1968. Anatomical changes in the neuromuscular complex of the proleg of Galleria mellonella (L.) (Lepidoptera: Pyralidiadae) during metamorphosis. Journal of Morphology 125:105–127.

Rattanachan, N., B. Boonsoong, P. Getwongsa, Y. Uttaruk, and S. Narumon. 2014. A Benthic Macroinvertebrate Multimetric Index for Assessment of the Ecological Integrity of Northeast Streams, Thailand. EnvironmentAsia 7:104–111.

Rebechi, D., and M. A. Navarro-Silva. 2012. Setting the reference for the use of Chironomus sancticaroli (Diptera: Chironomidae) as bioindicator: Ontogenetic pattern of larval head structures. Zoologia (Curitiba) 29:167–171.

Rech, K. C., R. M. Guereschi, K. H. Torres, and A. P. de O. Nuñer. 2014. Subsidies for production of Chironomus calligraphus larvae (Chironomidae, Diptera) in the laboratory. Invertebrate Reproduction & Development 58:199–206.

Reyes-Maldonado, R., B. Marie, and A. Ramírez. 2021. Rearing methods and life cycle characteristics of Chironomus sp. Florida (Chironomidae: Diptera): A rapid-developing species for laboratory studies. Plos one 16:1–16.

Richardi, V. S., G. S. Morais, M. A. Navarro-Silva, M. Vicentini, T. A. da Silva, L. F. Fávaro, and D. Rebechi. 2018. Effects of phenanthrene on different levels of biological organization in larvae of the sediment-dwelling invertebrate Chironomus sancticaroli (Diptera: Chironomidae). Environmental Pollution 242:277–287.

Richardi, V. S., D. Rebechi, J. M. R. Aranha, and M. A. Navarro-silva. 2013. Determination of larval instars in Chironomus sancticaroli (Diptera: Chironomidae) using novel head capsule structures. Zoologia 30:211–216.

Richardi, V. S., M. Vicentini, D. Rebechi, L. F. Fávaro, and M. A. Navarro-silva. 2015. Morpho-histological characterization of immature of the bioindicator midge Chironomus sancticaroli Strixino and Strixino (Diptera, Chironomidae). Revista Brasileira de Entomologia 59:240–250.

Ristola, T., J. Pellinen, M. Ruokolainen, A. Kostamo, and J. V. K. Kukkonen. 1999. Effect of sediment type, feeding level, and larval density on growth and development of a midge (Chironomus riparius). Environmental Toxicology and Chemistry 18:756–764.

Robertson, L., H. Chasiotis, V. Galperin, and A. Donini. 2014a. Allatostatin A-like immunoreactivity in the nervous system and gut of the larval midge Chironomus riparius: modulation of hindgut motility, rectal K+ transport and implications for exposure to salinity:3815–3822.

Robertson, L., H. Chasiotis, V. Galperin, and A. Donini. 2014b. Allatostatin A-like immunoreactivity in the nervous system and gut of the larval midge Chironomus riparius: modulation of hindgut motility, rectal K+ transport and implications for exposure to salinity. Journal of Experimental Biology 217:3815–3822.

Rodríguez Cruz, P. M., J. Cossins, D. Beeson, and A. Vincent. 2020. The Neuromuscular Junction in Health and Disease: Molecular Mechanisms Governing Synaptic Formation and Homeostasis. Frontiers in Molecular Neuroscience 13:1–22.

Runck, C. 2007. Macroinvertebrate production and food web energetics in an industrially contaminated stream. Ecological Applications 17:740–753.

Sahragard, A., and M. Rafatifard. 2010. Biology and effect of temperature on larval development time of Chironomus riparius Meigen (Diptera: Chironomidade) under laboratory conditions. Mun. Ent. Zool. 5:1025–1033.

Sanders, T., Y. Liu, V. Buchner, and P. B. Tchounwou. 2009. Neurotoxic effects and biomarkers of lead exposure: a review. Reviews on environmental health 24:15–46.

Sanhueza, M., A. Kubasik-Thayil, and G. Pennetta. 2016. Why quantification matters: characterization of phenotypes at the drosophila larval neuromuscular junction. JoVE (Journal of Visualized Experiments):e53821.

Scales, M. D. C., and P. F. Credland. 1978. Cell and Tissue The Ultrastructure of the Non-Neurosecretory Components in the Brain of the Midge , Chironomus riparius Mg . (Diptera : Nematocera) 366:355–366.

Senderovich, Y., and M. Halpern. 2013. The protective role of endogenous bacterial communities in chironomid egg masses and larvae. ISME Journal 7:2147–2158.

Shankland, D. L. 1965. Nerves and muscles of the pregenital abdominal segments of the American cockroach, Periplaneta americana (L.). Journal of Morphology 117:353–385.

Shilpa, O., K. P. Anupama, A. Antony, and H. P. Gurushankara. 2021. Lead (Pb) induced oxidative stress as a mechanism to cause neurotoxicity in Drosophila melanogaster. Toxicology 462:152959.

Sigrist, S. J., D. F. Reiff, P. R. Thiel, J. R. Steinert, and C. M. Schuster. 2003. Experience-dependent strengthening of Drosophila neuromuscular junctions. The Journal of neuroscience : the official journal of the Society for Neuroscience 23:6546–56.

Simmons, P. J. 1977. The neuronal control of Dragonfly flight. Australian National University.

Soler-Llavina, S. M., and J. R. Ortiz-Zayas. 2017. Emergent contaminants in the wastewater effluents of two highly populated tropical cities. Journal of Water and Health 15:873–884.

Spehar, R. L., R. L. Anderson, and J. T. Fiandt. 1978. Toxicity and bioaccumulation of cadmium and lead in aquatic invertebrates. Environmental Pollution (1970) 15:195–208.

Stevens, M. M. 1998. Development and survival of Chironomus tepperi Skuse (Diptera : Chironomidae) at a range of constant temperatures. Aquatic Insects 20:181–188.

Stocker, B., C. Bochow, C. Damrau, T. Mathejczyk, H. Wolfenberg, J. Colomb, C. Weber, N. Ramesh, C. Duch, and N. M. Biserova. 2018. Structural and molecular properties of insect type II motor axon terminals. Frontiers in systems neuroscience 12:5.

Strixino, G., and S. T. Strixino. 1985. A temperatura e o desenvolvimento larval de Chironomus sancticaroli (Diptera: Chironomidae). Revista Brasileira de Zoologia 3:177–180.

Strixino, S. T., and G. Strixino. 1981. Nova espécie do gênero Chironomus Meigen do sul do Brasil (Diptera: Chironomidae). Revista brasileira de entomologia 25:333–340.

Thurén, A., and P. Woin. 1991. Effects of Phthalate Esters on the Locomotor Activity of. Bull.: Environ. Contam. Toxicol 46:159–166.

Timmermans, K. R., W. Peeters, and M. Tonkes. 1992. Cadmium, zinc, lead and copper inChironomus riparius (Meigen) larvae (Diptera, Chironomidae): Uptake and effects. Hydrobiologia 241:119–134.

Tokeshi, M. 1995. Life cycles and population dynamics. Pages 225–268 *in* P. D. Armitage, editor. The Chironomidae: biology and ecology of non-biting midges. Springer.

Torres, N. I., X. Yu, I. Y. Padilla, R. E. Macchiavelli, R. Ghasemizadeh, D. Kaeli, J. F. Cordero, J. D. Meeker, A. N. Alshawabkeh, and A. Arbor. 2018. The influence of hydrogeological and anthropogenic variables on phthalate contamination in eogenetic karst groundwater systems. Environ Pollut. 237:298–307.

Trivinho-Strixino, S., and G. Strixino. 1989. Observações sobre a biologia da reprodução de um quironomídeo da região neotropical (Diptera, Chironomidae). Revista Brasileira de entomologia 33:207–216.

Tseng, I. L., Y. F. Yang, C. W. Yu, W. H. Li, and V. H. C. Liao. 2013. Phthalates induce neurotoxicity affecting locomotor and thermotactic behaviors and AFD neurons through oxidative stress in Caenorhabditis elegans. PLoS ONE 8.

Usherwood, P. N. R. 1994. Insect glutamate receptors. Pages 309–341 Advances in insect physiology. Elsevier.

Wang, T.-T., F.-L. Si, Z.-B. He, and B. Chen. 2018. Genome-wide identification, characterization and classification of ionotropic glutamate receptor genes (iGluRs) in the malaria vector Anopheles sinensis (Diptera: Culicidae). Parasites & vectors 11:1–12.

Warwick, W. F., J. Fitchko, P. M. McKee, D. R. Hart, and A. J. Burt. 1987. The incidence of deformities in Chironomus spp. from Port Hope harbour, Lake Ontario. Journal of Great Lakes Research 13:88–92.

Webb, R. M. T., and F. Gomez-Gomez. 1998. Synoptic survey of water quality and bottom sediments, San Juan Bay Estuary system, Puerto Rico, December 1994-July 1995:US Geological Survey Water Resources Investigation.

Weber, R. E., and S. N. Vinogradov. 2001. Nonvertebrate hemoglobins: Functions and molecular adaptations. Physiological Reviews 81:569–628.

Webster, R. G. 2018. Animal models of the neuromuscular junction, vitally informative for understanding function and the molecular mechanisms of congenital myasthenic syndromes. International Journal of Molecular Sciences 19:1326.

Williams KA, DWJ . Green, D. Paseoe, D.E. Gower. 1986 The acute toxicity of cadmium to different larval stages of Chironomus riparius (Diptera : Chironomidae) and its ecological significance for pollution regulation. :362–366.

Xing, X. J., Q. Rui, M. Du, and D. Y. Wang. 2009. Exposure to lead and mercury in young larvae induces more severe deficits in neuronal survival and synaptic function than in adult nematodes. Archives of Environmental Contamination and Toxicology 56:732–741.

Xu, J.-M., S.-H. Chou, Y. Zhang, M. Kumar, and S.-Y. Shen. 2021. Degradation of Dibutyl Phthalate Plasticizer in Water by High-Performance Iro2-Ta2O5/Ti Electrocatalytic Electrode. Catalysts 11:1368.

Zhang, X., X. Ding, and Q. Zhang. 2007. Effects of dibutyl phthalate on fecundity and life span of drosophila melanogaster. Chinese Journal of Public Health 23:303–304.

Zhang, Y., Y. Jiao, Z. Li, Y. Tao, and Y. Yang. 2021. Hazards of phthalates (PAEs) exposure: A review of aquatic animal toxicology studies. Science of the Total Environment 771:145418.

Zhong, Y., and Chun-Fang Wu. 2004. Neuronal Activity and Adenylyl Cyclase in Environment-Dependent Plasticity of Axonal Outgrowth in Drosophila. Journal of Neuroscience 24:1439–1445.

Zilli, F. 2008. Biometry and life cycle of Chironomus calligraphus Goeldi 1905 (Diptera, Chironomidae) in laboratory conditions. Interciencia 33:767–770.

Zilli, F., M. Marchese, and A. Paggi. 2009. Life cycle of Goeldichironomus holoprasinus goeldi (Diptera: Chironomidae) in laboratory. Neotropical Entomology 38:472–6.